

Some new properties of the PamPa scheme

Rémi Abgrall (*) , Yongle Liu (*) and Philipp Öffner (†)

(*)Institute of Mathematics, University of Zürich, 8057 Zürich, Switzerland

(†)Institute of Mathematics, Clausthal University of Technology, D-38678 Clausthal-Zellerfeld, Germany

remi.abgrall@math.uzh.ch, yongle.liu@math.uzh.ch, philipp.oeffner@tu-clausthal.de

Abstract

In this paper, we provide a few new properties of Active Flux (AF)/Point-Average-Moment Polynomial-interpreted (PamPa) schemes. First, we show, in full generality, that the AF/PamPa schemes can be interpreted in such a way that the discontinuous Galerkin (dG) scheme is one of their building blocks. Secondly we provide intrinsic bound preserving properties of the current variant of PamPa. This is also illustrated numerically. Last, we show, at least in one dimension, that the PamPa scheme has the summation by part (SBP) property.

1 Introduction.

Since the seminal work of P.L. Roe and his students, [1, 2, 3, 4, 5, 6], there has been a growing interest in the so-called Active Flux schemes, see e.g. [7, 8, 9, 10, 11, 12, 13, 14] for hyperbolic conservation laws,

$$\frac{\partial \mathbf{u}}{\partial t} + \operatorname{div} \mathbf{f}(\mathbf{u}) = 0, \mathbf{x} \in \Omega \subset \mathbb{R}^d, t \geq 0 \quad (1)$$

subjected to initial and boundary conditions. Bold letters will be used for vector valued functions. For example, the conserved variables will be denoted by bold letters (\mathbf{u}) when they belong to \mathbb{R}^p with $p > 1$, and non bold ones when $p = 1$. The flux is $\mathbf{f} = (f_1, \dots, f_d)$ is assumed to be at least C^1 , and defined on $\mathcal{D} \subset \mathbb{R}^p$. This set is called the invariant domain, for example in the case of the Euler equations, it is defined by imposing a strictly positive density and internal energy.

These schemes evolve simultaneously the average values and point values on the boundary of elements, that can be quads, triangles and polygons in several space dimensions, and intervals in 1D. In these papers, several progress have been made: we are now able to handle non linear cases without spurious oscillations. Very high order schemes have been developed, see e.g. [12, 15]. Conformal and non conformal meshes can be used [16, 14]. Several very intriguing properties have been noticed, and in our opinion partially explained: the schemes, at least in the Cartesian version, seems to have very interesting properties for the low Mach flows [8].

What is missing is to understand these properties: this is the motivation of this paper, or more precisely. The present paper will not answer all the questions, but to provide some new links to more classical schemes, and to show that some facts that were known in one dimension (see e.g. [13]) are not specific to one dimensional problems.

In this paper we are interested in three things. We first show the connection of the PamPa scheme with discontinuous Galerkin (dG) schemes. In a way, the PamPa scheme is a ...continuous discontinuous Galerkin scheme. We show that for the 1D and multi D version of the scheme, for any order and any type of elements (interval, and simplex in several dimensions).

The second contribution is about bound preservation. In [14] it was noticed that the behavior of the average values is always smoother than that of the point values. In this paper, we show several intrinsic bound preserving properties on the average values.

The last contribution is about summation by parts properties of the PamPa scheme in one dimension.

During the review process, we have been made aware of the reference [17] which has a non empty overlap with our section 2. This paper has been sent to ArXiv at the same time as we submitted posted this paper on ArXiv. In section 2, we go above third order accuracy, or the one dimensional or Cartesian setting, however the main idea of connecting the approximation of (2) to finite element method is essentially the same.

Our scheme has of course a strong connection to the Active Flux family of schemes. Indeed, one of us has been very much inspired by P.L. Roe’s work, and in particular the references we have listed above, and also personal discussions. He also had the opportunity to listen to Franco Brezzi’s talks at the ICM in 2014. This talk was about Virtual Finite Elements (VEM), and is a subset of [18]. The connections were obvious, in particular how functions were approximated. For that reason, and because we do not use exact evolution operators, but the method of line, we decided no to use the vocable of “active flux”, but something else: our flux is inactive, and “inactive flux” would not have been very respectful. The naming of PamPa was introduced in [13], and we have sticked to it since, even if the question of invariant domain preservation is not always central.

2 Reinterpretation of the PamPa scheme.

In this section, we describe how the PamPa scheme can be reinterpreted starting from the dG method.

In a first step, we show in one dimension and several dimensions that in each element, we can rewrite the dG method using standard duality tools of linear algebra, in the case of a linear with constant coefficient hyperbolic. This is done for segments in one dimension, and simplex in two dimensions. The extension to 3D is straightforward. Using this, we show that the PamPa scheme of [10, 19, 12] is nothing more, when using a Runge-Kutta (RK) time procedure than, for each RK cycle, one step of dG followed by a projection onto globally continuous approximations. The case of non linear problems is also described, and we discuss several projections.

2.1 Standard PamPa Scheme.

We consider a tessellation of the 1-D spatial domain Ω in non overlapping elements $I_{j+\frac{1}{2}} = [x_j, x_{j+1}]$ with uniform size $\Delta x_{j+1/2} = x_{j+1} - x_j$. For sake of simplicity, we consider the advection equation:

$$u_t + au_x = 0 \tag{2}$$

with $a > 0$. We will write the flux as $f(u) = au$.

In the standard third-order PamPa (or the so-called generalized AF) scheme, the solution of (2) is approximated by a globally continuous finite element polynomial expansion¹ u_h within each element $I_{j+\frac{1}{2}}$:

$$u_h^{j+1/2}(x) = u_j \varphi_0(\xi) + \bar{u}_{j+\frac{1}{2}} \varphi_1(\xi) + u_{j+1} \varphi_2(\xi), \quad \xi = \frac{x - x_j}{\Delta x_{j+1/2}}, \quad x \in I_{j+\frac{1}{2}}, \tag{3}$$

where the quadratic polynomial basis functions are

$$\varphi_0 = (1 - \xi)(1 - 3\xi), \quad \varphi_1 = 6\xi(1 - \xi), \quad \varphi_2 = \xi(3\xi - 2).$$

The PamPa scheme is, for all $j \in \mathbb{Z}$: the average values evolve with

$$\Delta x_{j+1/2} \frac{d\bar{u}_{j+1/2}}{dt} + a(u_{j+1} - u_j) = 0, \tag{4a}$$

and the point values with

$$\Delta x_{j+1/2} \frac{du_{j+1}}{dt} + a(2u_j + 4u_{j+1} - 6\bar{u}_{j+1/2}) = 0. \tag{4b}$$

¹Following the finite element convention, we use the subscript h to indicate a finite element approximation of a variable.

The rationale behind the relation for u_{j+1} is that one can approximate the spatial derivative of u_h at $x = x_{j+1}$ by using the approximation of u either on $I_{j+1/2}$ or $I_{j+3/2}$ or combinations of the derivatives. Since $a > 0$, we take the approximation using information from the downwind interval, i.e. $I_{j+1/2}$, so that

$$\frac{du_h^{j+1/2}}{dx}(x_{j+1}) = \frac{2u_j + 4u_{j+1} - 6\bar{u}_{j+1/2}}{\Delta x_{j+1/2}}.$$

If a were negative, the relation (4b) would be replaced by

$$\Delta x_{j+3/2} \frac{du_{j+1}}{dt} + a(6\bar{u}_{j+3/2} - 4u_{j+1} - 2u_{j+2}) = 0$$

or equivalently by

$$\Delta x_{j+1/2} \frac{du_j}{dt} + a(6\bar{u}_{j+1/2} - 4u_j - 2u_{j+1}) = 0.$$

Now, we reinterpret it as an dG scheme.

The mass matrix \mathbf{M} given by $M_{i,j} = \int_{x_j}^{x_{j+1}} \varphi_i(\xi)\varphi_j(\xi)d\xi$ is

$$\mathbf{M} = \Delta x_{j+1/2} \begin{pmatrix} \frac{2}{15} & -\frac{1}{10} & -\frac{1}{30} \\ -\frac{1}{10} & \frac{6}{5} & -\frac{2}{10} \\ -\frac{1}{30} & -\frac{1}{10} & \frac{2}{15} \end{pmatrix} \quad (5)$$

and its inverse is

$$\mathbf{M}^{-1} = \frac{1}{\Delta x_{j+1/2}} \begin{pmatrix} 9 & 1 & 3 \\ 1 & 1 & 1 \\ 3 & 1 & 9 \end{pmatrix} \quad (6)$$

in each element $I_{j+\frac{1}{2}}$. On the other hand, we have the following update procedure

$$\begin{aligned} \int_{I_{j+\frac{1}{2}}} \varphi_0\left(\frac{x-x_j}{\Delta x_{j+1/2}}\right)u_h'(x) dx &= \bar{u}_{j+\frac{1}{2}} - \frac{u_j + u_{j+1}}{2}, \\ \int_{I_{j+\frac{1}{2}}} \varphi_2\left(\frac{x-x_j}{\Delta x_{j+1/2}}\right)u_h'(x) dx &= u_{j+1} - u_j, \\ \int_{I_{j+\frac{1}{2}}} \varphi_1\left(\frac{x-x_j}{\Delta x_{j+1/2}}\right)u_h'(x) dx &= \frac{u_j + u_{j+1}}{2} - \bar{u}_{j+\frac{1}{2}}. \end{aligned} \quad (7)$$

So that, we get in total

$$\mathbf{M} \frac{d}{dt} \begin{pmatrix} u_j \\ \bar{u}_{j+\frac{1}{2}} \\ u_{j+1} \end{pmatrix} + a \begin{pmatrix} \bar{u}_{j+\frac{1}{2}} - \frac{u_j + u_{j+1}}{2} \\ u_{j+1} - u_j \\ \frac{u_j + u_{j+1}}{2} - \bar{u}_{j+\frac{1}{2}} \end{pmatrix} = 0, \quad (8)$$

which can be further written as, using (6):

$$\frac{d}{dt} \begin{pmatrix} u_j \\ \bar{u}_{j+\frac{1}{2}} \\ u_{j+1} \end{pmatrix} + \frac{a}{\Delta x_{j+1/2}} \begin{pmatrix} 6\bar{u}_{j+\frac{1}{2}} - 4u_j - 2u_{j+1} \\ u_{j+1} - u_j \\ 2u_j + 4u_{j+1} - 6\bar{u}_{j+\frac{1}{2}} \end{pmatrix} = 0. \quad (9)$$

We also note that

$$\frac{a}{\Delta x_{j+1/2}} \begin{pmatrix} 6\bar{u}_{j+\frac{1}{2}} - 4u_j - 2u_{j+1} \\ u_{j+1} - u_j \\ 2u_j + 4u_{j+1} - 6\bar{u}_{j+\frac{1}{2}} \end{pmatrix} = \begin{pmatrix} f'(u_j) \\ f(u_{j+1}) - f(u_j) \\ f'(u_{j+1}) \end{pmatrix}.$$

In the general case of $a \in \mathbb{R}$, we can interpret PamPa as follows:

1. Run dG as here,
2. Drop the update of u_j
 - if $a > 0$: coming from the interval $I_{j+\frac{1}{2}}$ and keep the internal DoFs computed from dG.
 - If $a < 0$, coming from the interval $I_{j-\frac{1}{2}}$ and keep the internal DoFs computed from dG.

2.2 High order PamPa scheme.

In the high order case, we take $m_i(x) = \left(\frac{x-x_j}{\Delta x_{j+1/2}}\right)^i$ in the interval $I_{j+\frac{1}{2}}$ and define the degrees of freedom (DoFs) for degree k (where the formal order of the scheme is $k+1$) as

$$u_0 \approx u(x_j), \quad u_1 \approx u(x_{j+1}), \quad u_{l+2} = \int_{I_{j+\frac{1}{2}}} m_l(x) u(x) dx, \quad \text{for } 0 \leq l \leq k-2. \quad (10)$$

Note that in (10), we have changed the ordering of the corresponding coefficients due to the high-order approach. We denote the linear forms as follows:

$$\langle \theta_l, u \rangle = u_l, \quad 0 \leq l \leq k$$

where θ_l is a bounded linear functional. We denote the dual basis in \mathbb{P}^k by $\{\varphi_q \in \mathbb{P}^k\}$, $q = 0, \dots, k$ such that $\langle \theta_l, \varphi_q \rangle = \delta_{lq}$. In $I_{j+\frac{1}{2}}$, $u(x)$ is approximated as

$$u_h(x) = \sum_{q=0}^k u_q \varphi_q(x). \quad (11)$$

In the PamPa method, we first compute the point value evolution equations

$$\begin{aligned} \frac{du_0}{dt} + a \frac{du_h}{dx}(x_j) &= 0, \\ \frac{du_1}{dt} + a \frac{du_h}{dx}(x_{j+1}) &= 0, \end{aligned} \quad (12a)$$

and for the moments for $0 \leq l \leq k-2$, we write

$$\frac{du_{l+2}}{dt} + \int_{I_{j+\frac{1}{2}}} a m_l(x) \frac{du_h}{dx} dx = 0. \quad (12b)$$

Using the same basis for \mathbb{P}^k , the dG method writes

$$\mathbf{M} \frac{d\mathbf{U}}{dt} + \mathbf{F} = 0$$

with $\mathbf{M}_{l\kappa} = \int_{I_{j+\frac{1}{2}}} \varphi_l(x) \varphi_\kappa(x) dx$ and

$$\mathbf{F}_\kappa = \int_{I_{j+\frac{1}{2}}} a \varphi_\kappa(x) \frac{du_h}{dx} dx.$$

The question is to compare them.

For this, using Riesz theorem, we can write $\langle \theta_l, u \rangle = (\psi_l, u)$ where

$$(u, v) = \int_{I_{j+\frac{1}{2}}} u(x) v(x) dx.$$

and $\psi_l \in \mathbb{P}^k$ again. Clearly, for $l \geq 0$, $\psi_{l+2} = m_l$. For $l = 0, 1$ (corresponding to the vertices x_j and x_{j+1}), we also write ψ_l as linear combinations of the φ_q s:

$$\psi_l = \sum_{q=0}^k a_{lq} \varphi_q$$

and from the orthogonality condition $\delta_{lp} = \langle \theta_l, \varphi_p \rangle = (\psi_l, \varphi_p)$,

$$\delta_{lp} = (\psi_l, \varphi_p) = \sum_{q=0}^k a_{lq} (\varphi_q, \varphi_p) = \sum_{q=0}^k a_{lq} \mathbf{M}_{qp}$$

that we interpret as saying that the inverse of \mathbf{M} is the matrix (a_{lq}) .

Then we compute $\mathbf{M}^{-1}\mathbf{F}$ in a component-wise manner, and get

$$\begin{aligned} (\mathbf{M}^{-1}\mathbf{F})_p &= \sum_{l=0}^k a_{pl} F_l = \sum_{l=0}^k a_{pl} \int_{I_{j+\frac{1}{2}}} a_{\varphi_l} \frac{du_h}{dx} dx \\ &= a \times \int_{I_{j+\frac{1}{2}}} \left(\sum_{l=0}^k a_{pl} \varphi_l \right) \frac{du_h}{dx} dx \\ &= a \times \int_{I_{j+\frac{1}{2}}} \psi_p \frac{du_h}{dx} dx. \end{aligned} \tag{13}$$

The last step is to show that

$$a \int_{I_{j+\frac{1}{2}}} \psi_p \frac{du_h}{dx} dx = a \frac{du_h}{dx}(x_{j+p})$$

for $p = 0, 1$, i.e. the two linear forms associated with the points values. This is indeed the fact if $a \in \mathbb{R}$ is a constant and since $\frac{du_h}{dx} \in \mathbb{P}^k$ if $u_h \in \mathbb{P}^k$.

This shows that we recover the PamPa that we can again interpret as

1. Run dG as here,
2. Drop the update of u_j
 - if $a > 0$: coming from the interval $I_{j+\frac{1}{2}}$ and keep the internal DoFs computed from dG.
 - If $a < 0$, coming from the interval $I_{j-\frac{1}{2}}$ and keep the internal DoFs computed from dG.

2.3 PamPa for triangles.

We consider the scalar problem $u_t + \operatorname{div} \mathbf{f} = 0$ and the case of a triangle K . We want that the approximation space contains \mathbb{P}^k for the accuracy. We denote the vertices by \mathbf{a}_i , $i = 1, 2, 3$ and λ_i the barycentric coordinates of K . The DoFs are these vertices and the other $k - 1$ Gauss–Lobatto points on the three edges, and the $k(k - 1)/2$ additional moments [14]. All of these DoFs assemble the approximation space with dimension $N_{\text{DoFs}} = 3 + 3(k - 1) + k(k - 1)/2 = 3k + k(k - 1)/2$.

The dimension of \mathbb{P}^k is $(k + 1)(k + 2)/2$. The number of Lagrange points on each edge, taking into account the vertices as Lagrange points, is $3k$. We have

$$3k + k(k - 1)/2 - 3k = \frac{k(k - 1)}{2} = \dim \mathbb{P}^{k-2}.$$

These equalities can be rephrased as follows. We set $B_{\boldsymbol{\mu}} = c_{\boldsymbol{\mu}} \lambda_1^{\mu_1} \lambda_2^{\mu_2} \lambda_3^{\mu_3}$ the Bézier polynomials. For the sake of simplicity, we will write

$$\lambda_1^{\mu_1} \lambda_2^{\mu_2} \lambda_3^{\mu_3} = \boldsymbol{\lambda}^{\boldsymbol{\mu}}.$$

The multi-index $\boldsymbol{\mu}$ is $\boldsymbol{\mu} = (\mu_1, \mu_2, \mu_3)$. We set $|\boldsymbol{\mu}| = \mu_1 + \mu_2 + \mu_3$. The coefficients $c_{\boldsymbol{\mu}}$ are binomial coefficients so that the $B_{\boldsymbol{\mu}}$ s can be seen as the terms in the development of $(\lambda_1 + \lambda_2 + \lambda_3)^k$. We define the two vector spaces:

$$V_1 = \text{span}\{B_{\boldsymbol{\mu}}, |\boldsymbol{\mu}| = k \text{ and } \mu_1\mu_2\mu_3 = 0\}$$

and

$$V_2 = \text{span}\{B_{\boldsymbol{\mu}}, |\boldsymbol{\mu}| = k \text{ and } \mu_1\mu_2\mu_3 > 0\}.$$

Clearly, $\mathbb{P}^k \subset V_1 \oplus V_2$. The elements of V_2 vanish on the boundary of K . For the sake of clarity, we will denote the generator of V_2 with a specific notation

$$\psi_{\boldsymbol{\mu}} = \lambda_1\lambda_2\lambda_3 B_{\boldsymbol{\mu}}$$

with

- if $1 \leq k \leq 2$, $B_{\boldsymbol{\mu}} = 1$,
- and for $k \geq 3$, $B_{\boldsymbol{\mu}} = \boldsymbol{\lambda}^{\boldsymbol{\mu}}$ with

$$|\boldsymbol{\mu}| = k - 2.$$

It is clear that $\dim V_1 = 3k$ and $\dim V_2 = \dim \mathbb{P}^{k-2}$. We define

$$\mathcal{I}_k = \begin{cases} \{\boldsymbol{\mu}, |\boldsymbol{\mu}| = k - 2\} & \text{for } k > 2 \\ \{(0, 0, 0)\} & \text{for } k \leq 2. \end{cases}$$

The cardinal of \mathcal{I}_k is $\dim \mathbb{P}^{k-2}$. We will often write $b = \lambda_1\lambda_2\lambda_3$.

We introduce the following polynomial spaces:

- For $k \leq 2$, $V = \mathbb{P}^k \oplus b\mathbb{R}$,
- and for $k > 2$, $V = \mathbb{P}^k \oplus b\mathbb{P}^{k-2}$

We introduce the following degrees of freedom:

- For the Gauss-Lobatto points σ on the boundary of K ,

$$\langle \delta_{\sigma}, p \rangle = p(\sigma). \tag{14a}$$

The set of Gauss-Lobatto points is denoted by \mathcal{G} and contains $3k$ points.

- In the interior,

$$\langle m_{\boldsymbol{\mu}}, p \rangle = \frac{1}{|K|} \int_K \boldsymbol{\lambda}^{\boldsymbol{\mu}}(\mathbf{x}) p(\mathbf{x}) \, d\mathbf{x} \tag{14b}$$

for $\boldsymbol{\mu} \in \mathcal{I}_k$.

They are linear forms on V .

Lemma 2.1. *The linear forms (14a)-(14b) are uni-solvent on V .*

Proof. Let α_{σ} , $\sigma \in \mathcal{G}$ and $\alpha_{\boldsymbol{\mu}'}$, $\boldsymbol{\mu}' \in \mathcal{I}_k$ be real numbers such that for all $p \in V$

$$\sum_{\sigma \in \mathcal{G}} \alpha_{\sigma} \langle \delta_{\sigma}, p \rangle + \sum_{\boldsymbol{\mu}' \in \mathcal{I}_k} \alpha_{\boldsymbol{\mu}'} \langle m_{\boldsymbol{\mu}'}, p \rangle = 0. \tag{15}$$

We first consider the Lagrange polynomials L_{σ} at σ and define

$$\varphi_{\sigma} = L_{\sigma} - \sum_{\boldsymbol{\mu} \in \mathcal{I}_k} \frac{m_{\boldsymbol{\mu}}(L_{\sigma})}{m_{\boldsymbol{\mu}}(\psi_{\boldsymbol{\mu}})} \psi_{\boldsymbol{\mu}} \tag{16}$$

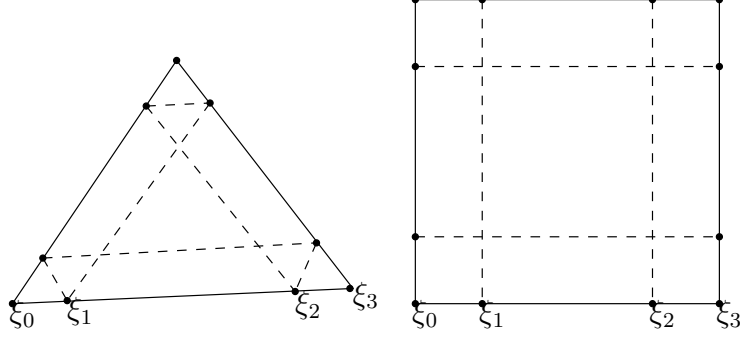


Figure 1: Interpolation points for the triangular and quadrangular, cubic case.

Since $\psi_{\boldsymbol{\mu}}$ vanishes on ∂K and L_{σ} is a Lagrange polynomial for the Gauss-Lobatto points, we have

$$\langle \delta_{\sigma'}, \varphi_{\sigma} \rangle = \delta_{\sigma'}^{\sigma'}$$

and by construction, for all $\boldsymbol{\mu} \in \mathcal{I}_k$,

$$\langle m_{\boldsymbol{\mu}}, \varphi_{\sigma} \rangle = 0.$$

Using this to test (15), we see that $\alpha_{\sigma} = 0$ for $\sigma \in \mathcal{G}$.

Then we test with $p = \psi_{\boldsymbol{\mu}}$, $\boldsymbol{\mu} \in \mathcal{I}_k$, that is

$$\sum_{\boldsymbol{\mu}' \in \mathcal{I}_k} \alpha_{\boldsymbol{\mu}'} \int_K \lambda_1 \lambda_2 \lambda_3 \boldsymbol{\lambda}^{\boldsymbol{\mu}'} \boldsymbol{\lambda}^{\boldsymbol{\mu}} \, d\mathbf{x} = 0. \quad (17)$$

The question reduces to that of the invertibility of the $|\mathcal{I}_k| \times |\mathcal{I}_k|$ symmetric matrix

$$A = \left(\int_K \lambda_1 \lambda_2 \lambda_3 \boldsymbol{\lambda}^{\boldsymbol{\mu}'} \boldsymbol{\lambda}^{\boldsymbol{\mu}} \, d\mathbf{x} \right).$$

Taking $X \in \mathbb{R}^{|\mathcal{I}_k|}$, we see that

$$X^T A X = \int_K \lambda_1 \lambda_2 \lambda_3 \varphi^2(\mathbf{x}) \, d\mathbf{x}$$

with

$$\varphi = \sum_{\boldsymbol{\mu} \in \mathcal{I}_k} X_{\boldsymbol{\mu}} \boldsymbol{\lambda}^{\boldsymbol{\mu}}.$$

Since $\{\boldsymbol{\lambda}^{\boldsymbol{\mu}}\}_{\boldsymbol{\mu} \in \mathcal{I}_k}$ is free, the matrix is positive definite. Thus the forms are unisolvent. \square

The second step is to compute the dual basis of $\{\delta_{\sigma}, m_{\boldsymbol{\mu}}\}_{\sigma, \boldsymbol{\mu}}$, i.e. elements $\{\phi_{\sigma}, \phi_{\boldsymbol{\mu}}\}_{\sigma, \boldsymbol{\mu}}$ of V such that for all σ ,

$$\forall \sigma', \langle \delta_{\sigma}, \varphi_{\sigma'} \rangle = \delta_{\sigma}^{\sigma'} \text{ and } \forall \boldsymbol{\mu}, \langle \delta_{\sigma}, \varphi_{\boldsymbol{\mu}} \rangle = 0$$

and for all $\boldsymbol{\mu}$,

$$\forall \sigma, \langle m_{\boldsymbol{\mu}}, \varphi_{\sigma} \rangle = 0 \text{ and } \forall \boldsymbol{\mu}', \langle m_{\boldsymbol{\mu}}, \varphi_{\boldsymbol{\mu}'} \rangle = \delta_{\boldsymbol{\mu}}^{\boldsymbol{\mu}'}$$

We have the following lemma:

Lemma 2.2 (Dual basis). *The dual basis of the forms $\delta_{\sigma}, m_{\boldsymbol{\mu}}$ consists in the elements of V defined by:*

- Associated to the Gauss-Lobatto points, the family $\{\varphi_{\sigma}\}$ defined by (16).

- Associated to the moments: the elements $\varphi_{\boldsymbol{\mu}}$ defined by

$$\varphi_{\boldsymbol{\mu}} = \lambda_1 \lambda_2 \lambda_3 \left(\sum_{\boldsymbol{\nu} \in \mathcal{I}_k} a_{\boldsymbol{\mu}\boldsymbol{\nu}} \lambda^{\boldsymbol{\nu}} \right)$$

where the $\{a_{\boldsymbol{\mu}\boldsymbol{\nu}}\}$ are solution of the linear system

$$\boldsymbol{\alpha}(a_{\boldsymbol{\mu}\boldsymbol{\nu}}) = (\delta_{\boldsymbol{\mu}}^{\boldsymbol{\nu}}) = \mathbf{Id}_{|\mathcal{I}_k| \times |\mathcal{I}_k|}$$

with

$$\alpha_{\boldsymbol{\mu}, \boldsymbol{\nu}} = 2|K| \frac{(\mu_1 + \nu_1 + 1)!(\mu_2 + \nu_2 + 1)(\mu_3 + \nu_3 + 1)!}{(2k + 1)!}.$$

This matrix is positive definite.

- The coefficients $a_{\boldsymbol{\mu}\boldsymbol{\nu}}$ only depend on $\boldsymbol{\mu} + \boldsymbol{\nu}$, we write $a_{\boldsymbol{\mu}\boldsymbol{\nu}} = a_{\boldsymbol{\mu} + \boldsymbol{\nu}}$.

Proof. We need to define the $\varphi_{\boldsymbol{\mu}}$ s. Since $\langle \delta_{\sigma}, \varphi_{\boldsymbol{\mu}} \rangle = 0$ for all σ , we see that

$$\varphi_{\boldsymbol{\mu}} = \lambda_1 \lambda_2 \lambda_3 \left(\sum_{\boldsymbol{\nu} \in \mathcal{I}_k} a_{\boldsymbol{\mu}\boldsymbol{\nu}} \lambda^{\boldsymbol{\nu}} \right)$$

and from the second set of family, that for all $\boldsymbol{\nu}'$,

$$\sum_{\boldsymbol{\nu} \in \mathcal{I}_k} \alpha_{\boldsymbol{\mu}\boldsymbol{\nu}} \int_K \lambda_1 \lambda_2 \lambda_3 \lambda^{\boldsymbol{\nu}} \lambda^{\boldsymbol{\nu}'} \, d\mathbf{x} = \delta_{\boldsymbol{\mu}}^{\boldsymbol{\nu}'}$$

Looking at the matrix with general term

$$\alpha_{\boldsymbol{\mu}, \boldsymbol{\nu}} = \int_K \lambda_1 \lambda_2 \lambda_3 \lambda^{\boldsymbol{\mu}} \lambda^{\boldsymbol{\nu}} \, d\mathbf{x} = 2|K| \frac{(\mu_1 + \nu_1 + 1)!(\mu_2 + \nu_2 + 1)(\mu_3 + \nu_3 + 1)!}{(2k + 1)!}$$

because $\boldsymbol{\mu}, \boldsymbol{\nu} \in \mathcal{I}_k$ so that $2 + \sum_i \mu_i + \sum_i \nu_i + 3 = 2(k - 2) + 5 = 2k + 1$. For the same reason as above, this matrix is invertible because it is positive definite.

We also see that since $\alpha_{\boldsymbol{\mu}, \boldsymbol{\nu}}$ depends only on $\boldsymbol{\mu} + \boldsymbol{\nu}$, using for example Cramer's formula, we get that $a_{\boldsymbol{\mu}\boldsymbol{\nu}}$ only depends on $\boldsymbol{\mu} + \boldsymbol{\nu}$. \square

For example for $k = 3$ (which is the first non trivial example), we have, for the moment $m_{\boldsymbol{\mu}}$ with $\boldsymbol{\mu} = (\mu_1, \mu_2, \mu_3)$ where the $\mu_1 + \mu_2 + \mu_3 = 1$, all the μ_j s are all equal to 0 except for one which is equal to 1. This leads to

$$\varphi_{\boldsymbol{\mu}} = \lambda_1 \lambda_2 \lambda_3 (a_1^k \lambda_1 + a_2^k \lambda_2 + a_3^k \lambda_3).$$

The matrix

$$A = \frac{1}{6!} \begin{pmatrix} 6 & 4 & 4 \\ 4 & 6 & 4 \\ 4 & 4 & 6 \end{pmatrix}$$

is circulant. Since $X = (a_1, a_2, a_3)^T = \left(\frac{1800}{7}, -\frac{720}{7}, -\frac{720}{7} \right)^T$ is the solution of

$$AX = \begin{pmatrix} 1 \\ 0 \\ 0 \end{pmatrix}$$

the polynomials are

- Moment λ_1 : $\varphi_{(1,0,0)} = \lambda_1 \lambda_2 \lambda_3 (a_1 \lambda_1 + a_2 \lambda_2 + a_3 \lambda_3)$.
- Moment λ_2 : $\varphi_{(0,1,0)} = \lambda_1 \lambda_2 \lambda_3 (a_3 \lambda_1 + a_1 \lambda_2 + a_2 \lambda_3)$.

- Moment λ_3 : $\varphi_{(0,0,1)} = \lambda_1 \lambda_2 \lambda_3 (a_2 \lambda_1 + a_3 \lambda_2 + a_1 \lambda_3)$.

From Riesz theorem, we know that for any linear form φ^* defined on V , there exists an element $\varphi \in V$ such that for all $p \in V$,

$$\langle \varphi^*, p \rangle = \frac{1}{|K|} \int_K \varphi(\mathbf{x}) p(\mathbf{x}) \, d\mathbf{x}$$

because

$$(p, q) = \frac{1}{|K|} \int_K p(\mathbf{x}) q(\mathbf{x}) \, d\mathbf{x}$$

is a scalar product on V .

From its definition, m_μ for $\mu \in \mathcal{I}_k$ is associated to λ^μ since

$$\langle m_\mu, p \rangle = \frac{1}{|K|} \int_K \lambda^\mu p \, d\mathbf{x}.$$

We are interested in looking at ψ_σ such that for all $p \in V$,

$$\langle \delta_\sigma, p \rangle = \frac{1}{|K|} \int_K \psi_\sigma p \, d\mathbf{x}.$$

We write

$$\psi_\sigma = \sum_{\sigma' \in \mathcal{G}} \alpha_{\sigma\sigma'} \varphi_{\sigma'} + \sum_{\mu' \in \mathcal{I}_k} \alpha_{\sigma\mu'} \varphi_{\mu'} \quad (18a)$$

and

$$\lambda^\mu = \sum_{\sigma' \in \mathcal{G}} \alpha_{\mu\sigma'} \varphi_{\sigma'} + \sum_{\mu' \in \mathcal{I}_k} \alpha_{\mu\mu'} \varphi_{\mu'} \quad (18b)$$

and get

$$\begin{aligned} |K| \delta_{\sigma\sigma'} &= \sum_{\sigma'' \in \mathcal{G}} \alpha_{\sigma\sigma''} \int_K \varphi_{\sigma''} \varphi_{\sigma'} \, d\mathbf{x} + \sum_{\mu' \in \mathcal{I}_k} \alpha_{\sigma\mu'} \int_K \varphi_{\sigma''} \varphi_{\mu'} \, d\mathbf{x}, \\ 0 &= \sum_{\sigma'' \in \mathcal{G}} \alpha_{\sigma\sigma''} \int_K \varphi_{\mu} \varphi_{\sigma'} \, d\mathbf{x} + \sum_{\mu' \in \mathcal{I}_k} \alpha_{\sigma\mu'} \int_K \varphi_{\mu} \varphi_{\mu'} \, d\mathbf{x}, \\ 0 &= \sum_{\sigma'' \in \mathcal{G}} \alpha_{\mu\sigma''} \int_K \varphi_{\sigma''} \varphi_{\sigma'} \, d\mathbf{x} + \sum_{\mu' \in \mathcal{I}_k} \alpha_{\mu\mu'} \int_K \varphi_{\sigma''} \varphi_{\mu'} \, d\mathbf{x}, \\ |K| \delta_{\mu\mu'} &= \sum_{\sigma'' \in \mathcal{G}} \alpha_{\mu\sigma''} \int_K \varphi_{\mu} \varphi_{\sigma'} \, d\mathbf{x} + \sum_{\mu'' \in \mathcal{I}_k} \alpha_{\mu\mu''} \int_K \varphi_{\mu} \varphi_{\mu'} \, d\mathbf{x} \end{aligned}$$

that is

$$\begin{aligned} |K| \begin{pmatrix} \mathbf{Id}_{(3k) \times (3k)} & \mathbf{0}_{(3k) \times |\mathcal{I}_k|} \\ \mathbf{0}_{|\mathcal{I}_k| \times (3k)} & \mathbf{Id}_{|\mathcal{I}_k| \times |\mathcal{I}_k|} \end{pmatrix} &= \begin{pmatrix} (\alpha_{\sigma\sigma'})_{(3k) \times (3k)} & (\alpha_{\sigma\mu'})_{(3k) \times |\mathcal{I}_k|} \\ (\alpha_{\mu\sigma'})_{|\mathcal{I}_k| \times (3k)} & (\alpha_{\mu\mu'})_{|\mathcal{I}_k| \times |\mathcal{I}_k|} \end{pmatrix} \\ &\times \begin{pmatrix} \left(\int_K \varphi_{\sigma} \varphi_{\sigma'} \, d\mathbf{x} \right)_{(3k) \times (3k)} & \left(\int_K \varphi_{\sigma} \varphi_{\mu'} \, d\mathbf{x} \right)_{(3k) \times |\mathcal{I}_k|} \\ \left(\int_K \varphi_{\mu} \varphi_{\sigma'} \, d\mathbf{x} \right)_{|\mathcal{I}_k| \times (3k)} & \left(\int_K \varphi_{\mu} \varphi_{\mu'} \, d\mathbf{x} \right)_{|\mathcal{I}_k| \times |\mathcal{I}_k|} \end{pmatrix}. \end{aligned} \quad (18c)$$

i.e. the matrix of the coordinates of the basis $\{\psi_\sigma, \lambda^\mu\}$ is the inverse of the mass matrix (up-to a factor $1/|K|$).

Application to the convection problem with constant advection speed. Then we extend what has been done in one dimension. We start from the problem

$$\frac{\partial u}{\partial t} + \mathbf{a} \cdot \nabla u = 0$$

in K , assuming an initial condition in V . At $t = 0$, since \mathbf{a} is constant, and from the definition of the elements of V , $\mathbf{a} \cdot \nabla u \in V$, and then we have initially

$$\begin{aligned} \frac{\partial}{\partial t} \langle \delta_\sigma, u \rangle + \langle \delta_\sigma, \mathbf{a} \cdot \nabla u \rangle &= 0 \\ \frac{\partial}{\partial t} \langle m_\mu, u \rangle + \langle m_\mu, \mathbf{a} \cdot \nabla u \rangle &= 0 \end{aligned} \tag{19}$$

that we can equivalently write as

$$\begin{aligned} \frac{\partial}{\partial t} \int_K \psi_\sigma u \, d\mathbf{x} + \int_K \psi_\sigma \mathbf{a} \cdot \nabla u \, d\mathbf{x} &= 0 \\ \frac{\partial}{\partial t} \int_K \lambda^\mu u \, d\mathbf{x} + \int_K \lambda^\mu \mathbf{a} \cdot \nabla u \, d\mathbf{x} &= 0 \end{aligned} \tag{20}$$

Then using (18), and in particular (18c), we get

$$M \frac{d}{dt} \left(\int_K \varphi_\sigma u \, d\mathbf{x} \right) + \left(\int_K \varphi_\sigma \mathbf{a} \cdot \nabla u \, d\mathbf{x} \right) = 0 \tag{21}$$

Remark 2.3. *If, instead of writing the time continuous version of the problem, we would have had started from a semi-discretisation in time, for example the explicit Euler forward scheme,*

$$u^{n+1} = u^n + \Delta t \mathbf{a} \cdot \nabla u^n,$$

we would have got

$$M \left(\left(\int_K \varphi_\sigma u \, d\mathbf{x} \right)^{n+1} - \left(\int_K \varphi_\sigma u \, d\mathbf{x} \right)^n \right) + \Delta t \left(\int_K \varphi_\sigma \mathbf{a} \cdot \nabla u \, d\mathbf{x} \right) = 0.$$

This is maybe a more rigorous way to proceed.

The method can be reinterpreted as in one dimension. We start from the dG approximation, setting

$$u_h = \sum_\sigma \langle \delta_\sigma, u \rangle \varphi_\sigma + \sum_\mu \langle m_\mu, u \rangle \phi_\mu,$$

let this evolve in time by

$$M \frac{d}{dt} \mathbf{U} + \mathbf{F} = 0$$

with

$$\mathbf{U} = (\{\langle \delta_\sigma, u \rangle\}, \{\langle m_\mu, u \rangle\})^T$$

and $\mathbf{F} = (\{F_\sigma\}, \{F_\mu\})^T$ with

$$F_\sigma = - \int_K \nabla \varphi_\sigma \cdot \mathbf{f}(u_h) \, d\mathbf{x} + \oint_{\partial K} \varphi_\sigma \mathbf{f}(u_h) \cdot \mathbf{n} \, d\gamma$$

and

$$F_\mu = - \int_K \nabla \phi_\mu \cdot \mathbf{f}(u_h) \, d\mathbf{x} + \oint_{\partial K} \phi_\mu \mathbf{f}(u_h) \cdot \mathbf{n} \, d\gamma$$

and then we get

$$\frac{d\mathbf{U}}{dt} + M^{-1} \begin{pmatrix} F_\sigma \\ F_\mu \end{pmatrix} = 0.$$

Remark 2.4 (Scheme for quadrangles). *The calculations are the same once we have evaluated the basis functions. They can be evaluated in the same way as for triangles.*

Remark 2.5 (Scheme for Polygons). *The extension of [19] to polygons has been made in [14]. The extension of what has been done in this section to polygons is quite natural, and will be the topic of a future publication.*

2.4 Interpretation of the PamPa scheme.

Again, we are dealing with the linear advection equation, with a constant speed. We will introduce the flux, $\mathbf{f}(u) = \mathbf{a} u$. For the sake of simplicity, we reduce ourselves to the case of third order, i.e. DoFs are point values and average, and we discuss only the one dimensional and triangular cases for simplicity. In the triangular case, again λ_1, λ_2 and λ_3 are the barycentric coordinates. The dG scheme in one element writes

$$\mathbb{M}_K \frac{dU_K}{dt} + F = 0$$

where $U_K = (\{u_\sigma\}_{\sigma \in K}, \bar{u}_K)$ and $F = (\{F_\sigma\}_{\sigma \in K}, \bar{F}_K)$ with

$$\begin{aligned} F_\sigma &= - \int_K \nabla \varphi_\sigma \cdot \mathbf{f}(u_h) \, d\mathbf{x} + \int_{\partial K} \varphi_\sigma \mathbf{f}(u_h) \cdot \mathbf{n} \, d\gamma, \\ \bar{F}_K &= - \int_K \nabla \bar{\varphi} \cdot \mathbf{f}(u_h) \, d\mathbf{x} + \int_{\partial K} \bar{\varphi} \mathbf{f}(u_h) \cdot \mathbf{n} \, d\gamma \end{aligned}$$

The Euler forward is

$$U_{|K}^{n+1} = U_{|K}^n - \Delta t M_K^{-1} F_K \quad (22a)$$

We note that

$$M_K^{-1} = P_K = \frac{1}{|K|} \mathcal{P}$$

where the matrix \mathcal{P} does not depend on K , because we are using barycentric coordinate: this is as if working in the reference element. From (22a), and using the previous results, we see that the average evolves as

$$\bar{u}_K^{n+1} = \bar{u}_K^n - \frac{\Delta t}{|K|} \int_{\partial K} \mathbf{f}(u_h) \cdot \mathbf{n} \, d\gamma$$

and the point values as

$$u_{\sigma,K}^{n+1} = u_\sigma^n - \frac{\Delta t}{|K|} \left(\mathcal{P}^{-1} F_K \right)_\sigma$$

where, using the previous results, we have

$$\left(\mathcal{P}^{-1} F_K \right)_\sigma = \int_K \nabla \varphi_\sigma \cdot \mathbf{f}(u_h) \, d\mathbf{x} + \int_{\partial K} \varphi_\sigma \mathbf{f}(u_h) \cdot \mathbf{n} \, d\gamma = \mathbf{a} \cdot \nabla u_h(\sigma).$$

We have written $u_{\sigma,K}^{n+1}$ to emphasis that there are several values of u_σ at time $n+1$. At time t_n , we have data in V , so that we need to project the family $\{u_{\sigma,K}^{n+1}\}$ onto V . One possibility is then: change nothing for the average, and for the points we do:

$$u_\sigma^{n+1} = \sum_{K, \sigma \in K} \omega_{K,\sigma} u_{\sigma,K}^{n+1} \quad (22b)$$

with weight $\omega_{\sigma,K}$ that are assumed to be positive and satisfy

$$\sum_{K, \sigma \in K} \omega_{K,\sigma} = \mathbf{Id}$$

to define a projection. This amount to write

$$u_\sigma^{n+1} = u_\sigma^n - \Delta t \sum_{K, \sigma \in K} \frac{\omega_{K, \sigma}}{|K|} (\mathcal{P}^{-1} F_K)_\sigma.$$

The next question is how to choose the weights $\omega_{K, \sigma}$? Looking back at [10] with this interpretation, where the mesh is $\{x_j\}_{j \in \mathbb{Z}}$ and the elements are $K_{j+1/2} = [x_j, x_{j+1}]$, the choice amounts to be, for $\sigma = x_j$

$$\omega_{K_{j+1/2}, x_j} = \frac{a^+}{a^+ + (-a)^+}, \quad \omega_{K_{j-1/2}, x_j} = \frac{(-a)^+}{a^+ + (-a)^+},$$

that is

$$\omega_{K_{j+1/2}, x_j} = \text{sign}(a), \quad \omega_{K_{j-1/2}, x_j} = \text{sign}(-a).$$

However, other choices are certainly possible. It is easy to see that in 1D, there is an energy inequality when we project with a simple averaging procedure: assume now that the scheme writes

$$\mathbf{u}_j^{n+1} = \frac{\Delta_{j+1/2} u_{j,j+1/2}^{n+1} + \Delta_{j-1/2} u_{j,j-1/2}^{n+1}}{\Delta_{j+1/2} + \Delta_{j-1/2}}$$

with $\Delta_{l+1/2} = x_{l+1} - x_l$.

This defines an energy diagonal matrix, i.e. a norm, and one can show that

Proposition 2.6. *We have the following energy inequality*

$$\begin{aligned} \sum_j (\Delta_{j+1/2} + \Delta_{j-1/2}) (u_j)^2 &= \sum_j (\Delta_{j+1/2} + \Delta_{j-1/2}) \left(\frac{\Delta_{j+1/2} u_{j,j+1/2} + \Delta_{j-1/2} u_{j,j-1/2}}{\Delta_{j+1/2} + \Delta_{j-1/2}} \right)^2 \\ &\leq \sum_K \Delta_{j+1/2} \left((u_{j,j+1/2})^2 + (u_{j,j-1/2})^2 \right)^2 \end{aligned} \quad (23)$$

Proof. For any $A, B, \alpha, \beta \in \mathbb{R}$ with $\alpha, \beta \geq 0$ and $\alpha + \beta = 1$, we have

$$(\alpha A + \beta B)^2 = \alpha^2 A^2 + \beta^2 B^2 + 2\alpha\beta AB \leq \alpha^2 A^2 + \beta^2 B^2 + \alpha\beta(A^2 + B^2) = \alpha A^2 + \beta B^2$$

then setting

$$\begin{aligned} \beta_j^+ &= \frac{\Delta_{j+1/2}}{\Delta_{j+1/2} + \Delta_{j-1/2}}, \quad \alpha_j^- = \frac{\Delta_{j-1/2}}{\Delta_{j+1/2} + \Delta_{j-1/2}}, \quad \gamma_j = \Delta_{j+1/2} + \Delta_{j-1/2} \\ \sum_j \gamma_j u_j^2 &= \sum_j \gamma_j (\alpha_j^- u_{j,j-1/2} + \beta_j^+ u_{j,j+1/2})^2 \leq \sum_j \gamma_j (\alpha_j^-) (u_{j,j-1/2})^2 + (\beta_j^+) (u_{j,j+1/2})^2 \\ &= \sum_{K=[x_j, x_{j+1}]} \left(\gamma_j \beta_j^- (u_{j,j+1/2})^2 + \gamma_{j+1} \alpha_{j+1}^- (u_{j+1,j+1/2})^2 \right) \end{aligned}$$

Then,

$$\begin{aligned} \sum_j \gamma_j u_j^2 &= \sum_j \gamma_j (\alpha_j^- u_j^- + \beta_j^+ u_j^+)^2 \leq \sum_j \gamma_j (\alpha_j^-) (u_j^-)^2 + (\beta_j^+) (u_j^+)^2 \\ &= \sum_K \left(\gamma_j \beta_j^- (u_j^+)^2 + \gamma_{j+1} \alpha_{j+1}^- (u_{j+1}^+)^2 \right) \\ &\leq \sum_K \Delta_{j+1/2} \left((u_j^+)^2 + (u_{j+1}^+)^2 \right) \end{aligned}$$

because

$$\gamma_j \beta_j^+ = \Delta_{j+1/2} \frac{\Delta_{j+1/2}}{\Delta_{j-1/2} + \Delta_{j+1/2}} \leq \Delta_{j+1/2}$$

and

$$\gamma_j \alpha_{j+1}^- = \Delta_{j+1/2} \frac{\Delta_{j+1/2}}{\Delta_{j+3/2} + \Delta_{j+1/2}} \leq \Delta_{j+1/2}.$$

which is nothing more than (23) when $\mathbf{u}_j^\pm = \mathbf{u}_{j,j\pm 1/2}$, etc \square

This strategy, in 1D, is illustrated on figure 2 where the problem is that of the convection of $\cos(2\pi x)$ with constant speed. The plot shows on a 100 points grid the result after 10 and 100 periods compared to the exact solution. We see very little dispersion. In two dimensions, the choice (22b) with weights defining

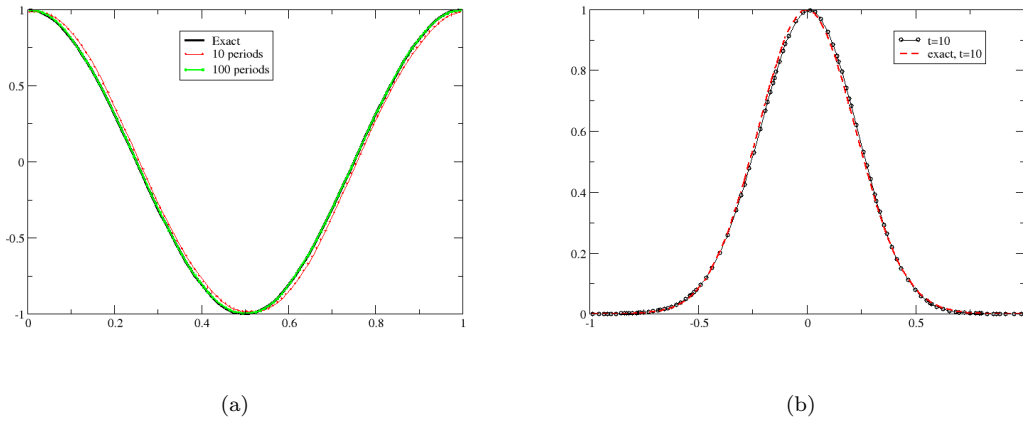


Figure 2: Solution of $u_t + u_x = 0$ with periodic boundary conditions on $[0, 1]$ for the initial condition $u_0 = \cos(2\pi x)$ after 10 and 100 periods, compared to the exact solution, on regular mesh (fig. a). On fig. (b), the initial solution is $u_0 = e^{-10x^2}$ on $[-1, 1]$ after 10 rotations on a random mesh.

an arithmetic average or an average weight by the area of the elements, as inspired by the 1D case, seems to lead to unstable results, but the choice

$$\tilde{\omega}_{\sigma,K} = \left(\sum_{K,\sigma \in K} (\text{sign}(\nabla \mathbf{f}(\mathbf{u}_\sigma) \cdot \mathbf{n}_\sigma^K) + \varepsilon \mathbf{Id}_k) \right)^{-1} \left(\text{sign}(\nabla \mathbf{f}(\mathbf{u}_\sigma) \cdot \mathbf{n}_\sigma^K) + \varepsilon \mathbf{Id}_k \right) \quad (24)$$

where, for $\mathbf{A} = (A, B)$, $A, B \in M_k(\mathbb{R})$ and $\mathbf{n} = (n_x, n_y)$, $\mathbf{A} \cdot \mathbf{n} = An_x + Bn_y$ and ε is a small positive parameter $\approx 10^{-20}$ to avoid inversion problems². This choice was made in [19], and then in [14] in the case of polygons.

This is illustrated by the following results, where, in $\Omega = [-20, 20]$,

$$\mathbf{u}_0(\mathbf{x}) = \exp(-\alpha \|\mathbf{x} - \mathbf{x}_0\|^2), \alpha = 0.25$$

on the problem

$$\frac{\partial \mathbf{u}}{\partial t} + \text{div} \mathbf{f}(\mathbf{u}) = 0 \quad (25)$$

²This can occur for example in the case where $\mathbf{f}(\mathbf{u}) = \mathbf{a}\mathbf{u}$, σ is the mid point of an edge parallel to \mathbf{a} . In that case up-winding makes no sense and the weight $\tilde{\omega}_\sigma$ is equal to $\frac{1}{2}$.

with

$$\mathbf{f}(u) = \mathbf{a}u, \quad \mathbf{a} = (-1, -1), \quad \mathbf{x}_0 = (15, 15) \quad (26a)$$

and final time $T = 30$ or

$$\mathbf{f}(\mathbf{x}, \mathbf{u}) = 2\pi(y, -x)u, \quad \mathbf{x} = (x, y), \quad \mathbf{x}_0 = (-10, 0) \quad (26b)$$

The final time is $T = 1$, i.e. one full rotation.

The tables 1 and 2 show the error for the scheme with upwind weights for (25) with the flux (26). The CFL is set to 0.3.

Average values						
h	L^1	slope	L^2	slope	L^∞	slope
0.4100	$0.4412 \cdot 10^{-3}$	-	$0.4412 \cdot 10^{-3}$	-	$0.4901 \cdot 10^{-1}$	-
0.2975	$0.1958 \cdot 10^{-3}$	2.533	$0.1224 \cdot 10^{-2}$	2.443	$0.2313 \cdot 10^{-1}$	2.341
0.2442	$0.1009 \cdot 10^{-3}$	3.361	$0.6420 \cdot 10^{-3}$	3.274	$0.1233 \cdot 10^{-1}$	3.189
0.2083	$0.5819 \cdot 10^{-4}$	3.460	$0.3732 \cdot 10^{-3}$	3.409	$0.7148 \cdot 10^{-2}$	3.429
0.1533	$0.2073 \cdot 10^{-4}$	3.364	$0.1347 \cdot 10^{-3}$	3.321	$0.2621 \cdot 10^{-2}$	3.270
Point values						
h	L^1	slope	L^2	slope	L^∞	slope
0.4100	$0.2915 \cdot 10^{-3}$	-	$0.2915 \cdot 10^{-3}$	-	$0.5018 \cdot 10^{-1}$	-
0.2975	$0.1295 \cdot 10^{-3}$	2.528	$0.1006 \cdot 10^{-2}$	2.456	$0.2338 \cdot 10^{-1}$	2.381
0.2442	$0.6689 \cdot 10^{-4}$	3.351	$0.5262 \cdot 10^{-3}$	3.285	$0.1238 \cdot 10^{-1}$	3.222
0.2083	$0.3863 \cdot 10^{-4}$	3.451	$0.3056 \cdot 10^{-3}$	3.416	$0.7208 \cdot 10^{-2}$	3.401
0.1533	$0.1379 \cdot 10^{-4}$	3.357	$0.1102 \cdot 10^{-3}$	3.325	$0.2633 \cdot 10^{-2}$	3.284

Table 1: Errors for the average and point values, triangular mesh, translation problem (25)-(26a) $T = 30$.

Average values						
h	L^1	slope	L^2	slope	L^∞	slope
0.4100	$0.4575 \cdot 10^{-3}$	-	$0.4575 \cdot 10^{-3}$	-	$0.7373 \cdot 10^{-1}$	-
0.2975	$0.3017 \cdot 10^{-3}$	1.297	$0.1883 \cdot 10^{-2}$	2.403	$0.3568 \cdot 10^{-1}$	2.262
0.2442	$0.1551 \cdot 10^{-3}$	3.376	$0.9853 \cdot 10^{-3}$	3.284	$0.1900 \cdot 10^{-1}$	3.197
0.2083	$0.8885 \cdot 10^{-4}$	3.500	$0.5702 \cdot 10^{-3}$	3.437	$0.1118 \cdot 10^{-1}$	3.334
0.1533	$0.3156 \cdot 10^{-4}$	3.375	$0.2042 \cdot 10^{-3}$	3.349	$0.4074 \cdot 10^{-2}$	3.290
Point values						
h	L^1	slope	L^2	slope	L^∞	slope
0.4100	$0.6794 \cdot 10^{-3}$	-	$0.6794 \cdot 10^{-3}$	-	$0.7538 \cdot 10^{-1}$	-
0.2975	$0.2034 \cdot 10^{-3}$	3.760	$0.1549 \cdot 10^{-2}$	2.436	$0.3596 \cdot 10^{-1}$	2.307
0.2442	$0.1041 \cdot 10^{-3}$	3.395	$0.8083 \cdot 10^{-3}$	3.298	$0.1922 \cdot 10^{-1}$	3.178
0.2083	$0.5968 \cdot 10^{-4}$	3.498	$0.4671 \cdot 10^{-3}$	3.446	$0.1125 \cdot 10^{-1}$	3.363
0.1533	$0.2115 \cdot 10^{-4}$	3.382	$0.2042 \cdot 10^{-3}$	2.699	$0.4084 \cdot 10^{-2}$	3.305

Table 2: Errors for the average and point values, triangular mesh, rotation problem (25)-(26b), $T = 1$.

This shows that the scheme delivers the expected error, even a little bit more. This is likely be a coincidence.

2.5 Generatisation to non constant advection speeds and non linear problems.

In [19] and [14], the update of the average is done by

$$|K| \frac{d\bar{u}_K}{dt} + \int_{\partial K} \mathbf{f}(u) \cdot \mathbf{n} \, d\gamma = 0,$$

while the update of the point values is done by

$$\frac{du_\sigma}{dt} + \sum_{K, \sigma \in K} \omega_{\sigma, K} \mathbf{J}(u_\sigma) \nabla u|_K(\boldsymbol{\sigma}) = 0$$

where \mathbf{J} is the Jacobian of the flux with respect to the conservative variables and $\omega_{\sigma, K}$ is obtained by a generalisation of (24), see [19, 14] for details. The main difference with the linear convection problem with constant speed is that $\text{div } \mathbf{f}(u)$ is not an element of V , so that the equivalence is lost. Nevertheless, one can extend what we have already written in that case, it will be a different scheme that needs to be studied. This interpretation of the PamPa scheme allows in particular to understand how to discretise boundary conditions, see [20] for such a study that is above the present contribution.

3 Intrinsic positivity properties of PamPa

In all the examples described bellow, as well as in [14], the solution of (1) is approximated by

$$\mathbf{u}_h = \sum_{\sigma \in \partial K} \mathbf{u}_\sigma \varphi_\sigma + \bar{\mathbf{u}}_K \bar{\varphi}_K$$

where

- $\bar{\varphi}_K = 0$ on ∂K , and $\int_K \bar{\varphi}_K \, d\mathbf{x} = |K|$,
- $\varphi_\sigma(\boldsymbol{\sigma}') = \delta_{\boldsymbol{\sigma}'}^{\boldsymbol{\sigma}}$, and for all σ ,

$$\int_K \varphi_\sigma \, d\mathbf{x} = 0$$

We will call $\bar{\varphi}$ a bubble function, and in each cases, it admits a maximum that we will denote by \mathbf{x}^* . This maximum is in the interior of the polygon.

In this section, we show the following result:

Proposition 3.1. *Let K be an element or a polygon. For the 1D third order scheme, the 2D quadratic, cubic, cubic moment and the scheme of [14], we have the following property: There exists $c_0 > 0$ depending only on K with the following property: If $\mathbf{u}_\sigma^n \in \mathcal{D}$ and $\mathbf{u}(\mathbf{x}^*) \in \mathcal{D}$ then*

$$\bar{\mathbf{u}}_K^{n+1} = \bar{\mathbf{u}}_K^n - \frac{\Delta t}{|K|} \oint_{\partial K} \mathbf{f}(\mathbf{u}_h) \cdot \mathbf{n} \, d\gamma$$

satisfies $\bar{\mathbf{u}}_K^{n+1} \in \mathcal{D}$ if

$$\Delta t \max_{\mathbf{x} \in K} \rho(\nabla \mathbf{f}(\mathbf{u}_h(\mathbf{x}))) \leq c_0 \frac{|K|}{|\partial K|}.$$

In order to establish this property, we proceed in 2 steps. First we show the following lemma

Lemma 3.2. *For the functional approximations mentioned in proposition 3.1, there exists $\mathbf{x}^* \in$ interior of K such that*

$$\mathbf{u}_h(\mathbf{x}^*) = \sum_{\sigma \in \partial K} \alpha_\sigma^K \mathbf{u}_\sigma + \omega_K \bar{u}_K$$

with

$$\omega_K > 0 \text{ and } \alpha_\sigma^K < 0.$$

In a second step, we use this property, which can be seen as a generalization of Simpson's formula, to established proposition 3.1.

In general we will have $\mathbf{u}(\mathbf{x}^*), \mathbf{u}_\sigma \in \mathcal{D}$ will imply that $\bar{u}_K \in \mathcal{D}$. But the converse is wrong. For example $u = 6x(1-x) + 7x(3x-2)$ is such that $u(0) = 0$, $u(1) = 7$ and $\bar{u} = 1$, but $u(1/2) = -1/4 < 0$. This means that when $u(\mathbf{x}^*) \notin \mathcal{D}$, something else must be done. One possibility is described in [14] where a monolithic convex limiting is used. Another possibility, getting inspiration from dG is to "limit" \mathbf{u} in K while keeping the average. Such a solution is described in [13], the price to pay is to use numerical flux to update the average value. What we conjecture is that a result of the type described in Lemma 3.2 is always true.

3.1 The 1D case.

We begin with the 1D case, repeating [13]. The computational domain is covered by a set of non-overlapping cells denoted by $I_{j+\frac{1}{2}} = [x_j, x_{j+1}]$ centered at $x_{j+\frac{1}{2}}$. The solution given in terms of boundary DoFs $u_j^n \approx u(x_j, t^n)$ and internal DoFs $\bar{u}_{j+\frac{1}{2}} \approx \int_{I_{j+\frac{1}{2}}} u(x) dx / \Delta x_{j+1/2}$ are assumed to be available. For each cell $I_{j+\frac{1}{2}}$, the internal DoF is evolved with

$$\bar{u}_{j+1/2}^{n+1} = \bar{u}_{j+1/2}^n - \lambda(f(u_{j+1}) - f(u_j)) \quad (27)$$

where $\lambda = \frac{\Delta t}{\Delta x_{j+1/2}}$ with Δx being the measure of the cell $I_{j+\frac{1}{2}}$ and Δt the adaptive time step depends on a certain CFL condition. We consider the third-order of accuracy here and thus can apply the Simpson's rule to write

$$\bar{u}_{j+1/2}^n = \frac{1}{6}(u_j^n + 4u_{j+1/2}^n + u_{j+1}^n),$$

so that (27) becomes

$$\begin{aligned} \bar{u}_{j+1/2}^{n+1} &= \frac{1}{6} \left(u_{j+1}^n - 6\lambda(f(u_{j+1}) - \hat{f}(u_{j+1}, u_{j+1/2})) \right) \\ &+ \frac{4}{6} \left(u_{j+1/2}^n - \frac{6}{4}\lambda(\hat{f}(u_{j+1}, u_{j+1/2}) - \hat{f}(u_{j+1/2}, u_j)) \right) \\ &+ \frac{1}{6} \left(u_j^n - 6\lambda(\hat{f}(u_{j+1/2}, u_j) - f(u_j)) \right) \end{aligned}$$

Then, we look at the intervals: in the cell $[x_{j-1}, x_j]$ we have 3 constant cells with value u_{j-1} , $u_{j-1/2}$, u_j and in the cell $[x_j, x_{j+1}]$, we have 3 constant cells with values u_j , $u_{j+1/2}$, u_{j+1} , so that we can interpret the term $f(u_j)$ as the flux $\hat{f}(u_j, u_j)$ between the most right subcell of $[x_{j-1}, x_j]$ and the most left subcell of $[x_j, x_{j+1}]$. This shows that if $6\lambda \leq c_0$ the CFL constant for the monotone flux \hat{f} , if $u_{j+1/2}$ is in the bounds $[m, M]$ as well as the other terms, then $\bar{u}_{j+1/2}^{n+1} \in [m, M]$. In the one dimensional cubic case, the bubble function is $6x(1-x)$ and it reaches its maximum for $x = \frac{1}{2}$.

The key points are

- The quadrature formula with positive weights,
- The continuity of the approximation at the boundaries of the cell,

3.2 The 2D case.

If we can find a point such that

$$u(\mathbf{x}^*) = \sum_{\text{Lagrange points}} \omega_\sigma u(\mathbf{x}_\sigma) + \omega_K \bar{u}_K$$

with $\omega_K > 0$ and $\omega_\sigma < 0$, we can repeat the same argument.

3.2.1 Polynomial case: quadratic and cubic cases of [19].

For quadratic approximation, we have

$$u_h(\mathbf{x}) = \sum_{\sigma} u(\mathbf{x}_{\sigma}) \varphi_{\sigma}(\mathbf{x}) + \bar{u}_K \bar{\varphi}_K(\mathbf{x})$$

with

$$\begin{aligned} \bar{\varphi}_K &= 60\lambda_1\lambda_2\lambda_3 \\ \varphi_{\sigma_i} &= (2\lambda_i - 1)\lambda_i, \quad i = 1, 2, 3 \end{aligned}$$

and

$$\varphi_{\sigma_4} = 4\lambda_1\lambda_2 - \frac{1}{3}\bar{\varphi}_K, \quad \varphi_{\sigma_5} = 4\lambda_2\lambda_3 - \frac{1}{3}\bar{\varphi}_K, \quad \varphi_{\sigma_6} = 4\lambda_3\lambda_1 - \frac{1}{3}\bar{\varphi}_K,$$

and we see that for the centroid \mathbf{x}_K ,

$$\bar{\varphi}_K(\mathbf{x}_K) = \frac{60}{27}, \quad \varphi_{\sigma_i} = -\frac{1}{9}, \quad i = 1, 2, 3; \quad \varphi_{\sigma_i}(\mathbf{x}_K) = \frac{4}{9} - \frac{20}{27} = -\frac{8}{27}, \quad i = 4, 5, 6$$

i.e.

$$u(\mathbf{x}_K) = \frac{20}{9}\bar{u}_K - \frac{1}{9}\sum_{i=1}^3 u_{\sigma_i} - \frac{8}{27}\sum_{i=4}^6 u_{\sigma_i}$$

from which we get

$$\bar{u}_K = \frac{9}{20}u(\mathbf{x}_K) + \frac{1}{20}\sum_{i=1}^3 u_{\sigma_i} + \frac{2}{15}\sum_{i=4}^6 u_{\sigma_i}.$$

For cubic approximation, we have

$$\varphi_{\sigma_i} = \frac{1}{2}\lambda_i(3\lambda_i - 1)(3\lambda_i - 2) - \frac{60}{30}\lambda_1\lambda_2\lambda_3, \quad i = 1, 2, 3$$

and

$$\begin{aligned} \varphi_{\sigma_4} &= \frac{9}{2}\lambda_1\lambda_2(3\lambda_1 - 1) - \frac{9}{2}\lambda_1\lambda_2\lambda_3, & \varphi_{\sigma_5} &= \frac{9}{2}\lambda_1\lambda_2(3\lambda_2 - 1) - \frac{9}{2}\lambda_1\lambda_2\lambda_3, \\ \varphi_{\sigma_6} &= \frac{9}{2}\lambda_2\lambda_3(3\lambda_2 - 1) - \frac{9}{2}\lambda_1\lambda_2\lambda_3, & \varphi_{\sigma_7} &= \frac{9}{2}\lambda_2\lambda_3(3\lambda_3 - 1) - \frac{9}{2}\lambda_1\lambda_2\lambda_3, \\ \varphi_{\sigma_8} &= \frac{9}{2}\lambda_3\lambda_1(3\lambda_3 - 1) - \frac{9}{2}\lambda_1\lambda_2\lambda_3, & \varphi_{\sigma_9} &= \frac{9}{2}\lambda_3\lambda_1(3\lambda_1 - 1) - \frac{9}{2}\lambda_1\lambda_2\lambda_3, \end{aligned}$$

and we see that

$$u(\mathbf{x}_K) = -\sum_{j=1}^3 \frac{2}{27}u(\sigma_j) - \sum_{i=4}^9 \frac{1}{6}u(\sigma_i) + \frac{60}{27}\bar{u}_K.$$

From this we get

$$\bar{u}_K = \frac{9}{20}u(\mathbf{x}_K) + \frac{1}{30}\sum_{j=1}^3 u(\sigma_j) + \frac{9}{120}\sum_{i=4}^9 u(\sigma_i).$$

We note that

$$\frac{9}{20} + \frac{3}{20} + \frac{6}{15} = 1$$

and

$$\frac{9}{20} + \frac{3}{30} + \frac{54}{120} = 1.$$

3.2.2 Polynomial case: cubic moment.

We write

$$u_h(\mathbf{x}) = \sum_{\sigma \in \partial K} u_\sigma \varphi_\sigma(\mathbf{x}) + \sum_{\mu} m_\mu(u) \bar{\varphi}_\mu(\mathbf{x})$$

and we evaluate this at the centroid. Because the coefficients defining the $\bar{\varphi}_\mu$ are obtained by cyclic permutation, from lemma 2.2, we see that

$$\bar{\varphi}_\mu\left(\frac{1}{3}, \frac{1}{3}, \frac{1}{3}\right) = \frac{1}{3^P} \sum_{\nu} a_{\mu+\nu}$$

where P only depends on the degree ($P = 3 + (k - 2)$). This relation shows that

$$\omega_K = \varphi_\mu\left(\frac{1}{3}, \frac{1}{3}, \frac{1}{3}\right)$$

does not depend on μ and, because the sum of the moments is the average, we obtain

$$u_h\left(\frac{1}{3}, \frac{1}{3}, \frac{1}{3}\right) = \sum_{\sigma} u_\sigma \varphi_\sigma\left(\frac{1}{3}, \frac{1}{3}, \frac{1}{3}\right) + \omega_K \bar{\mathbf{u}}_K$$

The only thing to check is if $\omega_K > 0$ and

$$\varphi_\sigma\left(\frac{1}{3}, \frac{1}{3}, \frac{1}{3}\right) < 0.$$

In the cubic case ($k = 3$), $P = 4$ and

$$\omega_K = \frac{1}{3^4} \left(\frac{1800 - 720 - 720}{7} \right) = \frac{360}{7 \times 3^4} = \frac{360}{567} > 0$$

and $\varphi_\sigma\left(\frac{1}{3}, \frac{1}{3}, \frac{1}{3}\right) = P_\sigma\left(\frac{1}{3}, \frac{1}{3}, \frac{1}{3}\right) - \sum_{\mu} \frac{m_\mu(P_\sigma)}{m_\mu(\varphi_\mu)} \varphi_\mu\left(\frac{1}{3}, \frac{1}{3}, \frac{1}{3}\right)$. The Gauss-Lobatto points in $[0, 1]$ are $\{\alpha_0 = 0, \alpha_1 = \frac{\sqrt{5}-1}{2\sqrt{5}}, \alpha_2 = \frac{\sqrt{5}+1}{2\sqrt{5}}, \alpha_3 = 1\}$. The Lagrange polynomials are (the interpolation points are given by their barycentric coordinates)

- for $(1, 0, 0)$,

$$P_0 = \frac{\lambda_1(\lambda_1 - \alpha_1)(\lambda_1 - \alpha_2)}{(1 - \alpha_1)(1 - \alpha_2)}$$

and its value at the centroid is

$$-\frac{1}{27} < 0.$$

- For $(\alpha_2, \alpha_1, 0)$, it is

$$P_1 = \frac{\lambda_1 \lambda_2 (\lambda_1 - \alpha_1)}{\alpha_2 \alpha_1 (\alpha_2 - \alpha_1)}$$

and its value at the centroid is

$$\frac{5}{18} - \frac{5\sqrt{5}}{54} > 0$$

- for $(\alpha_1, \alpha_2, 0)$ it is

$$P_2 = \frac{\lambda_1 \lambda_2 (\lambda_1 - \alpha_2)}{\alpha_1 \alpha_2 (\alpha_1 - \alpha_2)}$$

and its value at the centroid is

$$\frac{5}{18} + \frac{5\sqrt{5}}{54} > 0$$

- for $(0, 1, 0)$,

$$P_3 = \frac{\lambda_2(\lambda_2 - \alpha_1)(\lambda_2 - \alpha_2)}{(1 - \alpha_1)(1 - \alpha_2)}$$

and its value at the centroid is

$$-\frac{1}{27} < 0.$$

Next, we know the value $\varphi_{\boldsymbol{\mu}}(\frac{1}{3}, \frac{1}{3}, \frac{1}{3}) = \frac{360}{567}$ from lemma 2.2 and the form of $\varphi_{\boldsymbol{\mu}}$. Moreover, we can compute $m_{\boldsymbol{\mu}}(\varphi_{\boldsymbol{\mu}})$ and $m_{\boldsymbol{\mu}}(P_{\boldsymbol{\sigma}})$. Finally, $\varphi_{\boldsymbol{\sigma}}(\frac{1}{3}, \frac{1}{3}, \frac{1}{3}) < 0$ is verified. So again we have the positivity.

3.2.3 Approximation using Virtual finite element (VEM) approximation

In [14] has been extended the method developed in [19]. The computational domain is covered by a family of non overlapping polygons denoted by K , $\Omega = \cup K$. In each polygon, the solution is approximated by an element of

$$V_k(K) = \{v \text{ such that } v|_{\partial K} \in \mathbb{P}^k(\partial K) \text{ and } \Delta v \in \mathbb{P}^{k-2}(K)\},$$

where $k \geq 2$. In Ω , the solution will be approximated in

$$V_k(\Omega) = \left(\bigoplus_K V_k(K) \right) \cap C^0(\Omega).$$

This kind of approximation was introduced in [18, 21, 22] in a variational framework. This is an extension of the classical finite element techniques, where the “elements” are no longer simplex but general polygons with very mild assumptions on the polygons (essentially that they are star shaped with respect to one point). Hence there is no longer a reference element, so that basis functions must be designed for each polygons. This is theoretically possible, at least analytically, but very cumbersome. Hence the idea behind VEM is to avoid to explicitly use basis functions. We sketch the framework, some more details are given in the appendix, the interested reader is suggested to study [18] for a review. The degrees of freedom are the Gauss-Lobatto points on each edge of K and the moments

$$m_{\boldsymbol{\mu}}(u) = \frac{1}{|K|} \int_K \left(\frac{\mathbf{x} - \mathbf{x}^*}{h_K} \right)^{\boldsymbol{\mu}} u(\mathbf{x}) \, d\mathbf{x}, \quad |\boldsymbol{\mu}| \leq k - 2$$

where we have introduced the following notations:

- \mathbf{x}^* is a point toward which K is star-shaped,
- $\boldsymbol{\mu} = (\mu_1, \dots, \mu_d)$ is a multi-index, $|\boldsymbol{\mu}| = \sum_{i=1}^d \mu_i$.
- If $\mathbf{y} = (y_1, \dots, y_d)$,

$$y^{\boldsymbol{\mu}} = \prod_{i=1}^d y_i^{\mu_i}.$$

- σ is any of the Gauss-Lobatto points.
- In the following π is the L^2 projector defined on $V_k(K)$ onto $\mathbb{P}^k(K)$, see [21, 22]. It is computable solely with the given DoFs, and there is no need to know the basis functions.
- We use the following notations for the “basis” functions: for each DoF on the boundary, we call $\varphi_{\boldsymbol{\sigma}}$ the element of $V_k(K)$ such that

$$\varphi_{\boldsymbol{\sigma}}(\boldsymbol{\sigma}') = \delta_{\boldsymbol{\sigma}'}^{\boldsymbol{\sigma}}, m_{\boldsymbol{\mu}}(\varphi_{\boldsymbol{\sigma}}) = 0, \quad \forall \boldsymbol{\mu}, |\boldsymbol{\mu}| \leq k - 2$$

and by $\varphi_{\boldsymbol{\mu}}$ the element of $V_k(K)$ such that

$$\forall \boldsymbol{\sigma}, \varphi_{\boldsymbol{\mu}}(\boldsymbol{\sigma}) = 0 \text{ and } m_{\boldsymbol{\mu}'}(\varphi_{\boldsymbol{\mu}}) = \delta_{\boldsymbol{\mu}'}^{\boldsymbol{\mu}}.$$

The question we want to address is that of the existence of generalised Simpson rules for polygons which are not assumed to be convex but assumed to be star shaped with respect to one point in K . This case is a bit more involved, and we consider the quadratic case only. Again we have on the polygon K

$$u_h(\mathbf{x}) = \sum_{\sigma \in \partial K} u(\mathbf{x}_\sigma) \varphi_\sigma(\mathbf{x}_\sigma) + \bar{u}_K \bar{\varphi}_K(\mathbf{x})$$

where the ‘‘basis’’ functions φ are such that:

- $\Delta \varphi_\sigma = \alpha_\sigma \in \mathbb{R}$, $\Delta \bar{\varphi}_K = \alpha_K \in \mathbb{R}$,
- $\bar{\varphi}_K = 0$ on ∂K and $\int_K \bar{\varphi}_K \, d\mathbf{x} = |K|$,
- $\varphi_\sigma(\sigma') = \delta_{\sigma'}^{\sigma'}$, $\varphi_\sigma \in \mathbb{P}^2(\partial K)$ and $\int_K \varphi_\sigma \, d\mathbf{x} = 0$.

The idea is to find a point $\mathbf{x}^* \in \overset{\circ}{\Omega}$ such that

$$u(\mathbf{x}^*) = \sum_{\sigma \in \partial \Omega} u_\sigma \varphi_\sigma(\mathbf{x}^*) + \bar{u} \bar{\varphi}_K(\mathbf{x}^*)$$

where

$$\bar{\varphi}_K(\mathbf{x}^*) > 0 \text{ and } \bar{\varphi}_\sigma(\mathbf{x}^*) < 0 \quad \forall \sigma \in \partial K.$$

It is easy to show that $\bar{\varphi}_K \geq 0$ on K . First $\alpha_K < 0$ because

$$\alpha_K |K| = \int_K \bar{\varphi}_K \Delta \bar{\varphi}_K \, d\mathbf{x} = - \int_K \nabla \bar{\varphi}_K^2 \, d\mathbf{x} + \int_{\partial K} \bar{\varphi}_K \nabla \bar{\varphi}_K \cdot \mathbf{n} \, d\gamma = - \int_K \nabla \bar{\varphi}_K^2 \, d\mathbf{x} < 0$$

and then $\Delta \bar{\varphi}_K = \alpha_K < 0$, so that the maximum principle shows that $\bar{\varphi} \geq 0$ on K . If \mathbf{x} is in the interior of K , the same maximum principle (more precisely the mean value theorem) shows that $\bar{\varphi}_K(\mathbf{x}) > 0$.

We call \mathbf{x}^* a point for which $\max_{\mathbf{x} \in \overset{\circ}{\Omega}} \bar{\varphi}_K(\mathbf{x}) = \bar{\varphi}_K(\mathbf{x}^*)$. We have $\mathbf{x}^* \in \overset{\circ}{\Omega}$ and $\bar{\varphi}_K(\mathbf{x}^*) > 1$ because, since

$$|K| \bar{\varphi}_K(\mathbf{x}^*) \geq \int_K \bar{\varphi}_K(\mathbf{x}) \, d\mathbf{x} = |K|,$$

we see that $\bar{\varphi}_K(\mathbf{x}^*) \geq 1$ and if $\bar{\varphi}_K(\mathbf{x}^*) = 1$, we would have

$$0 = \int_K \bar{\varphi}_K(\mathbf{x}) \, d\mathbf{x} - |K| = \int_K (\bar{\varphi}_K(\mathbf{x}) - 1) \, d\mathbf{x}$$

with $\bar{\varphi}_K(\mathbf{x}) - 1 \leq 0$, so $\bar{\varphi}_K(\mathbf{x}) - 1 = 0$ and this is not possible.

Next we show that $\alpha_\sigma > 0$. Let \mathbf{y}_σ a point where φ_σ reaches its minimum. It must be such that $\varphi_\sigma(\mathbf{y}_\sigma) < 0$ because

$$\int_K \varphi_\sigma(\mathbf{x}) \, d\mathbf{x} = 0.$$

We have two cases to look at:

- If σ is a midpoint, then $\varphi_\sigma \geq 0$ on the boundary. If $\alpha_\sigma \leq 0$, then from the maximum principle, $\varphi_\sigma \geq 0$ on Ω and then we cannot have

$$\int_K \varphi_\sigma(\mathbf{x}) \, d\mathbf{x} = 0.$$

So $\alpha_\sigma > 0$.

- If σ is a vertex: Assume that $\alpha_\sigma < 0$.

If $\Delta\varphi_\sigma = \alpha_\sigma < 0$, then we take $u = \varphi_\sigma + \theta\bar{\varphi}_K$ with $\theta > 0$. If the minimum of φ_σ is reached on the boundary, call it \mathbf{y}^* : $\min_\Omega \varphi_\sigma = \min_{\partial\Omega} \varphi_\sigma = \varphi_\sigma(\mathbf{y}^*)$. We have, because $\bar{\varphi}_K \geq 0$, $u \geq \varphi_\sigma$, so $\min_\Omega u \geq \min_\Omega \varphi_\sigma$. If the minimum of u is reached on $\partial\Omega$

$$\begin{aligned}\varphi_\sigma(\mathbf{y}^*) &= \min_\Omega \varphi_\sigma = \min_{\partial\Omega} \varphi_\sigma = \min_{\partial\Omega} (\varphi_\sigma + \theta\bar{\varphi}_K) \geq \min_\Omega (\varphi_\sigma + \theta\bar{\varphi}_K) \\ &= \varphi_\sigma(\mathbf{y}_\theta^*) + \theta\bar{\varphi}_K(\mathbf{y}_\theta^*) > \varphi_\sigma(\mathbf{y}_\theta^*),\end{aligned}$$

so this is absurd. Hence, we must have $\mathbf{y}^* \notin \partial\Omega$, so since it is a strict minimum, $\Delta\varphi_\sigma(\mathbf{y}^*) = \alpha_\sigma > 0$.

We want to show that $\varphi_\sigma(\mathbf{x}^*) < 0$.

We take $\varepsilon > 0$ and consider $\bar{\varphi}_\varepsilon = \log(\bar{\varphi}_K + \varepsilon)$. It is well defined, and we have

$$\nabla\bar{\varphi}_\varepsilon = \frac{\nabla\bar{\varphi}_K}{\bar{\varphi}_K + \varepsilon}, \nabla^2\bar{\varphi}_\varepsilon = -\frac{\nabla\bar{\varphi}_K \otimes \nabla\bar{\varphi}_K}{(\bar{\varphi}_K + \varepsilon)^2} + \frac{\nabla^2\bar{\varphi}_K}{\bar{\varphi}_K + \varepsilon},$$

so that

$$\Delta\bar{\varphi}_\varepsilon = -\frac{\|\nabla\bar{\varphi}_K\|^2}{(\bar{\varphi}_K + \varepsilon)^2} + \frac{\Delta\bar{\varphi}_K}{\bar{\varphi}_K + \varepsilon} \leq 0.$$

Then we consider $u = \varphi_\sigma + \theta_\varepsilon\bar{\varphi}_\varepsilon$ for $\theta_\varepsilon \geq 0$. It is clear that for ε small enough, $u \leq 0$ on $\partial\Omega$ if $1 + \theta_\varepsilon \log \varepsilon \leq 0$ because $\varphi_\sigma \leq \max_{\mathbf{x} \in \Omega} \varphi_\sigma = 1$. So we look for ε_0 such that if $\varepsilon \leq \varepsilon_0$,

$$\Delta\varphi_\sigma + \theta_\varepsilon\Delta\bar{\varphi}_\varepsilon \leq 0$$

We have

$$\Delta\varphi_\sigma + \theta_\varepsilon\Delta\bar{\varphi}_\varepsilon = \underbrace{\alpha_\sigma}_{\geq 0} - \theta_\varepsilon \left(\underbrace{\frac{\|\nabla\bar{\varphi}_K\|^2}{(\bar{\varphi}_K + \varepsilon)^2} + \frac{|\alpha_P|}{\bar{\varphi}_K + \varepsilon}}_{\geq 0} \right) \leq 0$$

if

$$\theta_\varepsilon \left(\frac{\|\nabla\bar{\varphi}_K\|^2}{(\bar{\varphi}_K + \varepsilon)^2} + \frac{|\alpha_P|}{\bar{\varphi}_K + \varepsilon} \right) \geq \alpha_\sigma$$

so we need

$$\theta_\varepsilon \left(\frac{\min_\Omega \|\nabla\bar{\varphi}_K\|^2}{(\bar{\varphi}_K(\mathbf{x}^*) + \varepsilon)^2} + \frac{|\alpha_P|}{\bar{\varphi}_K(\mathbf{x}^*) + \varepsilon} \right) \geq \alpha_\sigma$$

Together with the condition on the boundary, we need: so we need

$$\theta_\varepsilon \left(\frac{\min_\Omega \|\nabla\bar{\varphi}_K\|^2}{(\bar{\varphi}_K(\mathbf{x}^*) + \varepsilon)^2} + \frac{|\alpha_P|}{\bar{\varphi}_K(\mathbf{x}^*) + \varepsilon} \right) \geq \alpha_\sigma \text{ and } \theta_\varepsilon \log \varepsilon \leq -1$$

i.e

$$\theta_\varepsilon \left(\frac{\min_\Omega \|\nabla\bar{\varphi}_K\|^2}{(\bar{\varphi}_K(\mathbf{x}^*) + \varepsilon)^2} + \frac{|\alpha_P|}{\bar{\varphi}_K(\mathbf{x}^*) + \varepsilon} \right) \geq \alpha_\sigma \text{ and } \theta_\varepsilon \log \left(\frac{1}{\varepsilon} \right) \geq 1 \quad (28)$$

Last we want that

$$\varphi_\sigma(\mathbf{x}^*) \leq -\theta_\varepsilon \log(\bar{\varphi}_K(\mathbf{x}^*) + \varepsilon)$$

with

$$\bar{\varphi}_K(\mathbf{x}^*) + \varepsilon > 1 \quad (29)$$

so with ε small enough. So we first choose ε to meet (29) and then we choose $\theta > 0$ so that (28) is met. This shows that $\varphi_\sigma(\mathbf{x}^*) < 0$.

All in all, we have

$$u(\mathbf{x}^*) = \omega_K \bar{u}_K + \sum_{\sigma \in \partial K} \omega_i u_{\sigma_i},$$

so that

$$\bar{u}_K = \frac{1}{\omega_K} u(\mathbf{x}^*) - \sum_{\sigma \in \partial K} \frac{\omega_i}{\omega_K} u_{\sigma_i}.$$

Since (take $u \equiv 1$)

$$1 = \omega_K + \sum_{\sigma \in \partial K} \omega_i,$$

we see that

$$\frac{1}{\omega_K} - \sum_{\sigma \in \partial K} \frac{\omega_i}{\omega_K} = \frac{1}{\omega_K} \left(1 - \sum_{\sigma \in \partial K} \omega_i\right) = \frac{\omega_K}{\omega_K} = 1.$$

3.3 Analysis

We assume that (28) is such that if $u_0(\mathbf{x}) \in \mathcal{D}$ for all $\mathbf{x} \in \mathbb{R}^d$ (or almost everywhere), then $u(\mathbf{x}, t) \in \mathcal{D}$ for all $\mathbf{x} \in \mathbb{R}^d, t > 0$.

In what follows, we assume

$$\bar{u}_K = \alpha_K u(\mathbf{x}_K) + \sum_{i=1}^N \alpha_i u(\sigma_i)$$

with $\alpha_K, \alpha_i > 0$. We note that

$$\alpha_K + \sum_{i=1}^N \alpha_i = 1,$$

We write ($\lambda = \frac{\Delta t}{|K|}$)

$$\begin{aligned} \bar{u}_K^{n+1} &= \bar{u}_K^n - \lambda \sum_{i=1}^N \mathbf{f}(u_{\sigma_i}) \cdot \mathbf{n}_i \\ &= \alpha_K u(\mathbf{x}_K) + \sum_{i=1}^N \alpha_i u(\sigma_i) - \lambda \sum_{i=1}^N \mathbf{f}(u_{\sigma_i}) \cdot \mathbf{n}_i \\ &= \alpha_K \left(u(\mathbf{x}_K) - \frac{\lambda}{\alpha_K} \sum_{i=1}^N \hat{\mathbf{f}}_{\mathbf{n}_i}(u_{\sigma_i}, u(\mathbf{x}_K)) \right) \\ &\quad + \sum_{i=1}^N \alpha_i \left(u(\sigma_i) - \frac{\lambda}{\alpha_i} \left[\hat{\mathbf{f}}_{\mathbf{n}_i}(u_{\sigma_i}, u_{\sigma_i}) \cdot \mathbf{n}_i - \hat{\mathbf{f}}_{\mathbf{n}_i}(u_{\sigma_i}, u(\mathbf{x}_K)) \right] \right) \end{aligned}$$

where $\hat{\mathbf{f}}_{\mathbf{n}}(\uparrow, \downarrow)$. Hence, if

$$\lambda \min(\alpha_K, \min_i \alpha_i) \leq \lambda_0$$

where λ_0 is the maximum stability parameter for $\hat{\mathbf{f}}_{\mathbf{n}}$. This shows that under this condition, if $\hat{\mathbf{f}}_{\mathbf{n}}$ is invariant domain preserving, if $\{u_{\sigma}^n \in \mathcal{D}\}$ and $\bar{u}_K^n \in \mathcal{D}$ then $\bar{u}_K^{n+1} \in \mathcal{D}$.

We note that there is no need to define any control volume, this is a purely algebraic property.

3.4 Numerical evidence

In order to illustrate this property, we have used the scheme of [14] on

$$\frac{\partial u}{\partial t} + \frac{\partial u}{\partial x} = 0$$

on Jiang-Shu problem with periodic boundary conditions, 300 mesh points, until $T = 2$ with $CFL = 0.15 < \frac{1}{6}$. The results are displayed in figure 3. In the original scheme of [14], the bound preserving strategy is applied both on the point values and the average values. We have tested the results above where we apply the BP strategy only on the point values. On figure 4, we consider the compressible Euler equations and show the result of the simulation Configuration 3 of Lax & Liu in [23], the initial condition is

$$(\rho, u, v, p) = \begin{cases} (\rho_1, u_1, v_1, p_1) = (1.5, 0, 0, 1.5) & \text{if } x \geq 1 \text{ and } y \geq 1, \\ (\rho_2, u_2, v_2, p_2) = (0.5323, 1.206, 0, 0.3) & \text{if } x \leq 1 \text{ and } y \geq 1, \\ (\rho_3, u_3, v_3, p_3) = (0.138, 1.206, 1.206, 0.029) & \text{if } x \leq 1 \text{ and } y \leq 1, \\ (\rho_4, u_4, v_4, p_4) = (0.5323, 0, 1.206, 0.3) & \text{if } x \leq 1 \text{ and } y \leq 1. \end{cases}$$

Here, the four states are separated by shocks. The domain is $[-2, 2]^2$. The solution at $t_f = 3$ is displayed in Figure 4. The mesh is 100×100 cells, i.e. with 120312 DoFs. The scheme is that of [14] where we have applied the bound preserving procedure on the point values only. The CFL is set to 0.1. The spatial approximation uses the Virtual Finite Element formulation. This is in perfect agreement with proposition 3.1.

4 Comment on the connection to summation-by-parts

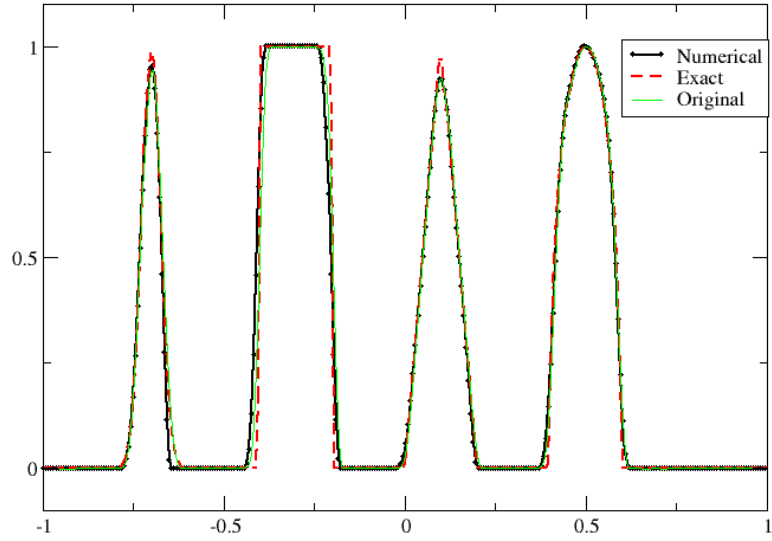
After our re-interpretation of the PamPa scheme in terms of dG, we are interested on the underlying structures/properties of the PamPa scheme even if we have shown that the scheme is energy stable. One key feature of numerical methods is the summation-by-parts (SBP) property. These schemes mimic integration-by-parts discretely and give a general framework to construct energy-stable schemes [24, 25, 26]. Several extensions exists of SBP operators, in addition, in [27], Mattesson introduced upwind SBP operators which have also been applied inside a dG framework together with flux vector splitting more recently in [28]. The key ingredients of SBP or upwind SBP are the following:

- The derivative matrix D which approximates the first derivative of a function and has to be exact up to a certain degree p of the underlying function space, normally polynomial approximation are used however it is not restricted to it, cf. [29]. In terms of upwind SBP operators, we have two operators D_+ and D_- which have to be exact up to a certain degree p of the polynomial vector space. They are constructed that $D = (D_+ + D_-)/2$ holds.
- In classical SBP and upwind SBP framework, a mass/norm matrix M which mimics the L^2 scalar product and often is set be a diagonal matrix where the entries on the diagonal are the quadrature weights. The exactness of the quadrature has to be at least $2p - 1$ for the construction process [30] if a polynomial approximation space is considered.
- The almost skew-symmetric matrix $Q := MD$ which fulfills than the SBP property meaning

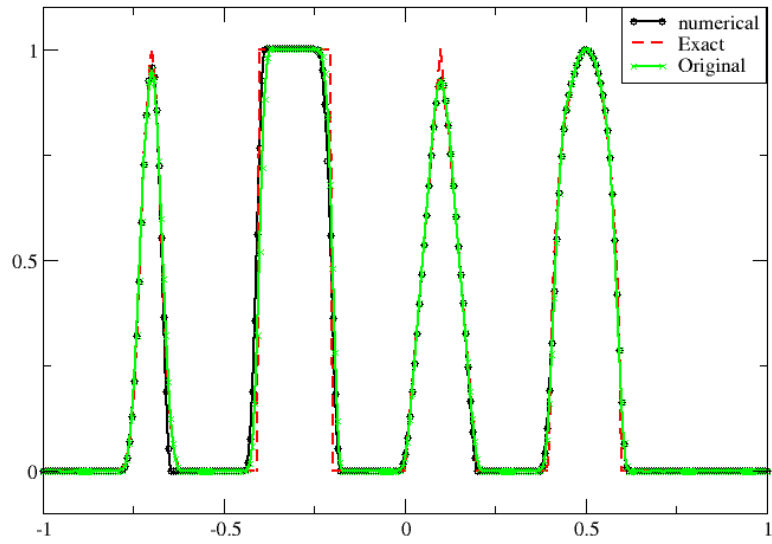
$$Q^T + Q = B = \text{diag}(-1, 0, \dots, 0, 1) \quad (30)$$

for inflow-outflow boundary conditions. For periodic boundary conditions, we have instead

$$Q^T + Q = 0. \quad (31)$$



(a)



(b)

Figure 3: Jiang and Shu's problem. (a): average values, (b): point values. Original: scheme of [14], Numerical: the BP strategy is applied only on the point values.

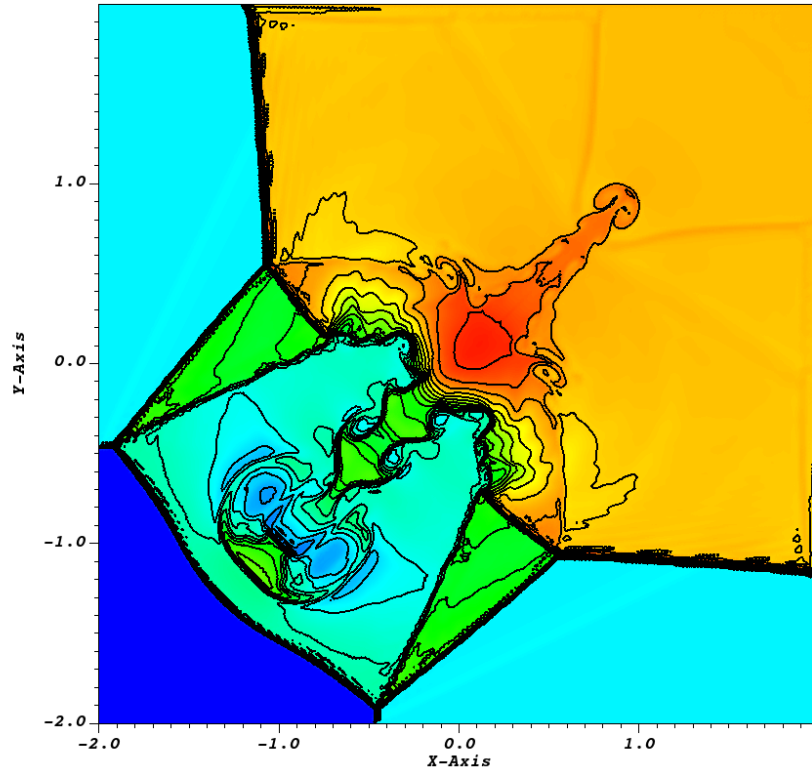


Figure 4: Solution of Lax-Liu case # 3.

In terms of the upwind SBP operators, we have Q_+ and Q_- such that $Q_+ + Q_-^T = 0$ and $Q_+ + Q_+^T = S$, where S is a dissipation matrix. S is symmetric and negative semi-definite. In the upwind case, we have therefore the following conditions:

$$\begin{aligned} D_+ &= M^{-1}(Q_+ + B/2) \text{ and } D_- = M^{-1}(Q_- + B/2), \\ MD_+ + D_-^T M^T &= B \text{ and } D_+ = D_- + M^{-1}S. \end{aligned} \quad (32)$$

Coming back to the PamPa (9) approach, we can directly define the almost skew-symmetric matrix Q from the SBP community using (7) in each element. It is given by

$$Q = \begin{pmatrix} -\frac{1}{2} & 1 & -\frac{1}{2} \\ -1 & 0 & 1 \\ \frac{1}{2} & -1 & \frac{1}{2} \end{pmatrix}$$

where $\mathbf{u} = (u_j, \bar{u}_{j+1/2}, u_{j+1})^T$. By direct calculation, (30) is naturally fulfilled with $B = \text{diag}(-1, 0, 1)$ where we have exactness for constants in the underlying function space due to

$$D\mathbf{1} = (M^{-1}Q)\mathbf{1} = \begin{pmatrix} -4 & 6 & -2 \\ -1 & 0 & 1 \\ 2 & -6 & 4 \end{pmatrix} \begin{pmatrix} 1 \\ 1 \\ 1 \end{pmatrix} = \mathbf{0}.$$

This is essential for local conservation [29]. The PamPa scheme fulfills essential all the properties which has been proven for SBP schemes or techniques which can be applied inside one element. However, up to this point this is now only the simple dG formulation with a non-classical approximation space. As it is described in previous chapters, the PamPa scheme is not like this, but use continuous approximations instead of the dG version. Therefore, we have now to project back from the discontinuous vector space to the continuous one. In terms of PamPa, we can do this via upwinding or central (or combination of them) at the point values at the element interfaces, cf. Section 2.4. It means for example when upwinding or a central projection is considered. We have the following cases:

- **Upwind:** Drop the update of u_j :
 - if $a > 0$: coming from the interval $I_{j+\frac{1}{2}}$ and keep the internal DoFs computed from dG.
 - If $a < 0$, coming from the interval $I_{j-\frac{1}{2}}$ and keep the internal DoFs computed from dG.
- **Central:** Take the average of the left and right contribution at the point values.

Therefore, we have to adapt the point value update in each element concerning the specific framework used where the average value $\bar{u}_{j+\frac{1}{2}}$ is not touched. Please remember that our vector inside the element $I_{j+\frac{1}{2}}$ for a third order method looks like this $(u_j, \bar{u}_{j+\frac{1}{2}}, u_{j+1})^T$ whereas inside $I_{j+\frac{3}{2}}$ we have $(u_{j+1}, \bar{u}_{j+\frac{3}{2}}, u_{j+2})^T$. Focusing on the common element interface at x_{j+1} , we have a value for u_{j+1}^- from the left calculated by the DoFs inside $I_{j+\frac{1}{2}}$ and alternatively one value from the right u_{j+1}^+ . Using (9), we have for the update of $u_{j+1}^{-/+}$ the following

$$\frac{d}{dt} \begin{pmatrix} u_j \\ \bar{u}_{j+\frac{1}{2}} \\ u_{j+1}^- \\ u_{j+1}^+ \\ \bar{u}_{j+\frac{3}{2}} \\ u_{j+2} \end{pmatrix} + \frac{a}{\Delta x} \begin{pmatrix} 6\bar{u}_{j+\frac{1}{2}} - 4u_j - 2u_{j+1}^- \\ u_{j+1}^- - u_j \\ 2u_j + 4u_{j+1}^- - 6\bar{u}_{j+\frac{1}{2}} \\ 6\bar{u}_{j+\frac{3}{2}} - 4u_{j+1}^+ - 2u_{j+1}^+ \\ u_{j+2} - u_{j+1}^+ \\ 2u_{j+1}^+ + 4u_{j+2} - 6\bar{u}_{j+\frac{3}{2}} \end{pmatrix} = 0. \quad (33)$$

This would be the dG update where we focus on the two neighboring elements $I_{j+\frac{1}{2}}$ and $I_{j+\frac{3}{2}}$. In this context, the update of u_{j+1} would be discontinuous over the element boundaries therefore we have to project back to the continuous approximation space. For simplicity reason later on, we select the central scheme.

approximation step. There are several possible ways to project, we have shown two, and mainly more are certainly possible: what is the "best" one, in which sense? This reformulation of PamPa leads to a generalisation to non linear problems. This generalisation is not equivalent to the formulation contained in [19] and [14] for non linear problem. In [34] this reformulation of PamPa has been used to formulated in a much better way the discretisation of boundary conditions. We have also show some intrinsic bound preserving properties of PamPa, linked to a generalisation of the Simpson formula. They have already been used in other publications to construct provable bound preserving schemes, and we also note that other solutions to the same problem are also available in the literature. Last, in one dimension, we have shown a SBP property of PamPa. One can imagine that a generalisation of this to multiD would provide an answer to the first question above: what is the "best" projection.

Acknowledgments.

We thank the many discussions we have had with Professor Kailiang Wu in SUSTech, China, in early June 2025. Y.L. was supported by UZH Postdoc Grant, 2024 / Verfügung Nr. FK-24-110 and SNFS grant 200020_204917 "Solving advection dominated problems with high order schemes with polygonal meshes: application to compressible and incompressible flow problems". P. Ö. is supported by the DFG within SPP 2410, project 525866748 and under the personal grant 520756621.

References

- [1] T.A. Eyman and P.L. Roe. Active flux. 49th AIAA Aerospace Science Meeting, 2011.
- [2] T.A. Eyman and P.L. Roe. Active flux for systems. 20 th AIAA Computational Fluid Dynamics Conference, 2011.
- [3] T.A. Eyman. *Active flux*. PhD thesis, University of Michigan, 2013.
- [4] T. A. Eymann and P. L. Roe. Multidimensional Active Flux schemes. In American Institute of Aeronautics and Astronautics, editors, *21st AIAA Computational Fluid Dynamics Conference*, 2013.
- [5] Jungyeoul Maeng. *On the Advective Component of Active Flux Schemes for Nonlinear Hyperbolic Conservation Laws*. PhD thesis, Applied and Interdisciplinary Mathematics, University of Michigan, 2017. <https://deepblue.lib.umich.edu/handle/2027.42/138695>.
- [6] Fanchen He. *Towards a New-generation Numerical Scheme for the Compressible Navier-Stokes Equations with the Active Flux Method*. PhD thesis, Applied and Interdisciplinary Mathematics, University of Michigan, 2021. <https://deepblue.lib.umich.edu/handle/2027.42/169687>.
- [7] W. Barsukow. The active flux scheme for nonlinear problems. *J. Sci. Comput.*, 86(1):Paper No. 3, 34, 2021.
- [8] Wasilij Barsukow, Jonathan Hohm, Christian Klingenberg, and Philip L. Roe. The active flux scheme on Cartesian grids and its low Mach number limit. *J. Sci. Comput.*, 81(1):594–622, 2019.
- [9] C. Helzel, D. Kerkmann, and L. Scandurra. A new ADER method inspired by the active flux method. *Journal of Scientific Computing*, 80(3):35–61, 2019.
- [10] R. Abgrall. A combination of residual distribution and the active flux formulations or a new class of schemes that can combine several writings of the same hyperbolic problem: application to the 1d Euler equations. *Commun. Appl. Math. Comput.*, 5(1):370–402, 2023.
- [11] R. Abgrall and Y. Liu. A new approach for designing well-balanced schemes for the shallow water equations: a combination of conservative and primitive formulations. *SIAM J. Sci. Comput.*, 46:A3375–A3400, 2024.

- [12] R. Abgrall and W. Barsukow. Extensions of active flux to arbitrary order of accuracy. *ESAIM, Math. Model. Numer. Anal.*, 57(2):991–1027, 2023.
- [13] Rémi Abgrall, Miaosen Jiao, Yongle Liu, and Kailiang Wu. Bound-preserving point-average-moment polynomial-interpreted (PAMPA) scheme: one-dimensional case. *Commun. Comput. Phys.*, 39(1):29–58, 2026. Preprint, arXiv:2412.03423 [math.NA] (2024).
- [14] R. Abgrall, W. Boscheri, and Y. Liu. Virtual finite element and hyperbolic problems: The PAMPA algorithm. *J. Comput. Phys.*, 546:114521, 2026. arXiv 2502.10069.
- [15] Wasilij Barsukow, Praveen Chandrashekar, Christian Klingenberg, and Lisa Lechner. A generalized active flux method of arbitrarily high order in two dimensions, 2025.
- [16] D. Calhoun, E. Chudzik, and C. Helzel. The Cartesian grid Active Flux method with adaptive mesh refinement. *J. Sci. Comput.*, 94:54, 2023.
- [17] Wasilij Barsukow. Semi-discrete active flux as a petrov-galerkin method, 2025.
- [18] Lourenço Beirão da Veiga, Franco Brezzi, L. Donatella Marini, and Alessandro Russo. The virtual element method. *Acta Numerica*, 32:123–202, 2023.
- [19] Rémi Abgrall, Jianfang Lin, and Yongle Liu. Active flux for triangular meshes for compressible flows problems. *Beijing J. of Pure and Appl. Math.*, 2:1–33, 2025.
- [20] Rémi Abgrall and Yongle Liu. Robust PAMPA Scheme in the DG Formulation on Unstructured Triangular Meshes: bound preservation, oscillation elimination, and boundary conditions. Preprint, arXiv:2511.16180 [math.NA] (2025), 2025.
- [21] L. Beirão da Veiga, Franco Brezzi, L. D. Marini, and A. Russo. The Hitchhiker’s guide to the virtual element method. *Math. Models Methods Appl. Sci.*, 24(8):1541–1573, 2014.
- [22] B. Ahmed, A. Alsaedi, F. Brezzi, L.D. Marini, and A. Russo. Projectors for Virtual Element Methods. *Comput. Math. Appl.*, 66(3), 2013.
- [23] Xu-Dong Liu and Peter D. Lax. Solution of two-dimensional riemann problems of gas dynamics by positive schemes. *SIAM J. Sci. Comput.*, 19:319–340, 1998.
- [24] David C. Del Rey Fernández, Jason E. Hicken, and David W. Zingg. Review of summation-by-parts operators with simultaneous approximation terms for the numerical solution of partial differential equations. *Comput. Fluids*, 95:171–196, 2014.
- [25] Magnus Svärd and Jan Nordström. Review of summation-by-parts schemes for initial-boundary-value problems. *J. Comput. Phys.*, 268:17–38, 2014.
- [26] R. Abgrall, J. Nordström, P. Öffner, and S. Tokareva. Analysis of the SBP-SAT stabilization for finite element methods. I: Linear problems. *J. Sci. Comput.*, 85(2):28, 2020. Id/No 43.
- [27] Ken Mattsson. Diagonal-norm upwind SBP operators. *J. Comput. Phys.*, 335:283–310, 2017.
- [28] Jan Glaubitz, Hendrik Ranocha, Andrew R. Winters, Michael Schlottke-Lakemper, Philipp Öffner, and Gregor Gassner. Generalized upwind summation-by-parts operators and their application to nodal discontinuous Galerkin methods. *J. Comput. Phys.*, 529:26, 2025. Id/No 113841.
- [29] Jan Glaubitz, Jan Nordström, and Philipp Öffner. Summation-by-parts operators for general function spaces. *SIAM J. Numer. Anal.*, 61(2):733–754, 2023.
- [30] David C. Del Rey Fernández, Pieter D. Boom, and David W. Zingg. A generalized framework for nodal first derivative summation-by-parts operators. *J. Comput. Phys.*, 266:214–239, 2014.

- [31] Pelle Olsson. Summation by parts, projections, and stability. I. *Math. Comput.*, 64(211):1035–1065, s23–s26, 1995.
- [32] Pelle Olsson. Summation by parts, projections, and stability. II. *Math. Comput.*, 64(212):1473–1493, 1995.
- [33] Wasilij Barsukow, Christian Klingenberg, Lisa Lechner, Jan Nordström, Sigrun Ortleb, and Hendrik Ranocha. Stability of the active flux method in the framework of summation-by-parts operators, 2025.
- [34] Rémi Abgrall and Yongle Liu. Robust PAMPA Scheme in the DG Formulation on Unstructured Triangular Meshes: bound preservation, oscillation elimination, and boundary conditions. Preprint, arXiv:2511.16180 [math.NA] (2025), 2025.

A VEM approximation: basic facts.

Any basis of $V_k(P)$ is virtual, meaning that it is not explicitly computed in closed form. Consequently, the evaluation of $v_h(\mathbf{x})$ at some $\mathbf{x} \in P$ it is not straightforward. One way to proceed would be to evaluate $\pi(v_h)$, that is the L^2 projection of v_h on $\mathbb{P}^k(P)$. Since we want to do it only using the degrees of freedom, it turns out that this is impossible in practice. But, as shown in [21, 22], it is possible to define a space $W_k(P)$ for which computing the L^2 projection is feasible. It is constructed from $V_k(P)$ in two steps. First, we consider the approximation space $\tilde{V}_k(P)$ given by

$$\tilde{V}_k(P) = \{v_h, v_h \text{ is continuous on } \partial P \text{ and } (v_h)_{\partial P} \in \mathbb{P}^k(\partial P); \text{ and } \Delta v_h \in \mathbb{P}^{k-2}(P)\}.$$

For $p \in \mathbb{N}$, let $M_p^*(P)$ be the vector space generated by the scaled monomial of degree p exactly,

$$m(\mathbf{x}) \in M_p^*(P), \quad m(\mathbf{x}) = \sum_{\alpha, |\alpha|=p} \beta_\alpha m_\alpha(\mathbf{x}).$$

Then, we consider $W_k(P)$, which is the subspace of $\tilde{V}_k(P)$ defined by

$$W_k(P) = \{w_h \in \tilde{V}_k(P), \langle w_h - \pi^\nabla w_h, q \rangle = 0, \quad \forall q \in M_{k-2}^*(P) \cup M_k^*(P)\}.$$

In [22], it is shown that $\dim V_k(P) = \dim W_k(P)$.

This approximation space is defined as follows. $w_h \in W_k(P)$ if and only if

1. w_h is a polynomial of degree k on each edge e of P , that is $(w_h)|_e \in \mathbb{P}^k(e)$,
2. w_h is continuous on ∂P ,
3. $\Delta w_h \in \mathbb{P}^{k-2}(P)$,
4. $\int_P w_h m_\alpha \, d\mathbf{x} = \int_P \pi^\nabla w_h m_\alpha \, d\mathbf{x}$ for $|\alpha| = k-1, k$.

The degrees of freedom are the same as in $V_k(P)$:

1. The value of w_h on the vertices of P ,
2. On each edge of P , the value of v_k at the $k-1$ internal points of the $k+1$ Gauss–Lobatto points on this edge,
3. The moments up to order $k-2$ of w_h in P ,

$$m_\alpha(w_h) := \frac{1}{|P|} \int_P w_h m_\alpha \, d\mathbf{x}, \quad |\alpha| \leq k-2.$$

The L^2 projection of w_h is computable. For any β , if $\pi^0(w_h) = \sum_{\alpha, |\alpha| \leq k} s_\alpha m_\alpha$, we have

$$\langle \pi^0(w_h), m_\beta \rangle = \sum_{\alpha, |\alpha| \leq k} s_\alpha \langle m_\beta, m_\alpha \rangle = \langle w_h, m_\beta \rangle.$$

The left hand side is computable since the inner product $\langle m_\beta, m_\alpha \rangle$ only involves monomials. We need to look at the right hand side. If $|\alpha| \leq k - 2$, $\langle w_h, m_\beta \rangle = |P| m_\beta(w_h)$ and if $|\alpha| = k - 1$ or k , we have

$$\langle w_h, m_\beta \rangle = \langle \pi^\nabla w_h, m_\alpha \rangle,$$

which is computable from the degrees of freedom only.

We note that if $w_h \in W_k(P)$, then $m_\alpha(\pi^0 w_h) = m_\alpha(w_h)$. Indeed

$$m_\alpha(\pi^0 w_h) = \frac{1}{|P|} \langle \pi^0 w_h, m_\alpha \rangle = \frac{1}{|P|} \langle w_h, m_\alpha \rangle$$

by construction. This is not true for π^∇ in $V_k(P)$. However, for $k \leq 2$, $V_k(P) = W_k(P)$

The last remark is that, since $\mathbb{P}^k(P) \subset V_k(P)$ and $\mathbb{P}^k(P) \subset W_k(P)$, the projections of $C^{k+1}(P)$ onto $V_k(P)$ and $W_k(P)$ defined by the degrees of freedom is $k + 1$ -th order accurate.

We recall how to approximate the mass matrix. We have for any i and j that represent the index of any degree of freedom,

$$\int_P \varphi_i \varphi_j = (\pi \varphi_i, \pi \varphi_j) + (\mathbf{Id} - \pi) \varphi_i, (\mathbf{Id} - \pi) \varphi_j$$

because for any $u \in L^2(K)$, we have,

$$((\mathbf{Id} - \pi)u, \pi v) = 0$$

The term

$$(\pi \varphi_i, \pi \varphi_j)$$

can be computed exactly, while we approximated

$$((\mathbf{Id} - \pi) \varphi_i, (\mathbf{Id} - \pi) \varphi_j) \approx |P| \sum_{r=1}^{N_{dof_s}} DOF_r((\mathbf{Id} - \pi) \varphi_i) DOF_r((\mathbf{Id} - \pi) \varphi_j)$$

The sum of the two matrices is invertible.